A Smart Bandage for the Automatic Detection and Treatment of *P. aeruginosa* Infections in Burns

by

David Hamdi
BEng, University of Victoria, 2017

A Thesis Submitted in Partial Fulfillment
Of the Requirements for the Degree of

Master of Applied Science

in the Department of Mechanical Engineering

Supervisory Committee

A Smart Bandage for the Automatic Detection and Treatment of P. Aeruginosa Infections in Burns.

by

David Hamdi
BEng, University of Victoria, 2017

Supervisory Committee

Dr. Mohsen Akbari, Mechanical Engineering
Supervisor

Dr. Yang Shi, Mechanical Engineering
Departmental Member

Abstract

Infection of thermal injuries by bacteria is a growing concern in the healthcare community, leading to increased rates of morbidity and mortality. *P. aeruginosa*, a rod-shaped, Gram-negative bacteria is one of the bacterial species most commonly found in infected burns. Detecting infections in burns is still a somewhat archaic process involving visual inspection, in which dressings have to be removed (also causing more pain and discomfort to patients) before samples are sent to a laboratory for analysis. Timely in situ detection systems, which limit disturbances to the wound area, could drastically improve patient comfort and healing outcomes. While established infections, with fully developed biofilms, are difficult to treat, loose bacteria early on in an infection and biofilm formation are more likely to fall easy prey to antibiotics, if the appropriate drugs are administered in a timely manner. In this thesis a smart wound management system, geared towards detecting and eliminating *P. aeruginosa* infections in burns is presented. Both non-functionalized general purpose electrodes, paired with an affordable open source potentiostat, for electrochemical analysis, and on demand drug releasing elements were developed by layering conductive materials onto everyday cotton threads. The sensing elements were thoroughly characterized with the detection of a *P. aeruginosa* biomarker over a range of physiologically relevant concentrations and conditions. The ability of the thread based sensors to detect live bacteria and be integrated in textile wound dressings was demonstrated. Controlled drug release was also demonstrated through the development of several drug release profiles. The presented technology has the potential to greatly improve patient outcomes in burn wards and provides a platform for tackling other infectious organisms with the further development of more thread based tools.

Table of Contents

List of Figures

List of Tables

Glossary

EPS - Extracellular Polymeric Substances

PBS - Phosphate Buffered Saline

DPBS - Dulbecco's Phosphate Buffered Saline

HaCaT - Immortal keratinocyte Cell line

LoB - Limit of Blank

LoD - Limit of Detection

SWV - Square Wave Voltammetry

PANI - Polyaniline

TSA - Tryptic Soy Agar

(w/v) - Percent weight per volume

PEGDA - Poly(Ethylene Glycol) DiAcrylate

ATP - Adenosine TriPhosphate

PDMS - PolyDiMethylSiloxane

SEM - Scanning Electron Microscope

FDA - Food and Drug Administration

PDI - PolyDispersity Index

NADPH - Nicotinamide Adenine DiNucleotide Phosphate

WHO - World Health Organization

S. epidermidis - *Staphylococcus epidermidis.*

B. cereus - *Bacillus cereus*

S. aureus - *Staphylococcus aureus*

E. coli - *Escherichia coli*

P. aeruginosa - *Pseudmonas aeruginosa*

Acknowledgments

First and foremost I would like to thank my supervisor Dr. Mohsen Akbari for his advice and guidance throughout this project and many others undertaken during my time at the Laboratory for Innovations in Micro Engineering (LIME). I will always be thankful for the opportunity he provided me in being part of his amazing lab and team.

Next, I would like to thank my fellow lab members without whom this work would not have been possible and my time as a graduate student at the University of Victoria wouldn't have been nearly as fun as it was. In particular I would like to thank Dr. Hosein Dabiri for his advice and assistance in carrying out experiments, Zhina Hadisi for her expertise in bacteria culture and animal work, Lucas Karperien for advice and knowledge of thread based sensors and Tavia Walsh for her aid with and discussion about electronics.

Lastly I would like to thank my parents Llew and Barb Hamdi, for always having my back. Without their support I would not be where I am today.

Dedication

I would like to dedicate this thesis to my parents Llew and Barb Hamdi. I thank you for setting me on this life long journey of learning. Your continued support has been instrumental in my academic achievements to date.

Chapter 1: Introduction

1.1 Why Burns are a Big Deal

Thermal injuries are a serious issue facing Canadians and the rest of the world. It has been estimated by the World Health Organization that roughly 188000 people pass away each year worldwide from burns [1]. In Canada alone for the 2009-2010 period there were roughly 127000 burn injuries reported nationwide [2]. Before delving further into the statistics surrounding burn injuries it is important to understand the pathophysiology of this type of injury. There are four degrees through which burns are classified with the first degree being the least severe and the fourth constituting the worst thermal injuries possible, based on the depth of the burn. The degrees of burn and their associated depth, appearance and feeling are summarized in Table 1 below. In addition to the degree of burn, based on the depth, burns over roughly 20% of the body can induce burn shock

Table 1: Degree of burns and their associated depth, appearance and feeling. [3]

Degree	Depth	Appearance	Feeling
1st	Only affects the epidermis	Red	Painful and Dry
2nd	Epidermis and part of the Dermis	Red and Blistered	Swollen and Painful
3rd	Full destruction of the Epidermis and Dermis with possible permeation into the subcutaneous tissue	White, Black or Charred	-
4th	Possibly permeates all the way to muscle or even bone.	-	No pain as the nerves have been destroyed

There are several avenues through which thermal injuries occur, including those induced through scalding, contact, flame and electrical burns. Scalding is burns through liquid, often boiling water or oil. Contact is through touching a hot object, such as a stove top. Flame induced burns are from anything with an open flame, such as a fireplace. Lastly electrical burns can be subdivided into occurrences in which current does or does not pass directly through the body [4]. Scalding accounts for 52.3% of burns in Canada while contact, flame and electrical burns account for 29.9%, 11.0% and 4.8% of burn injuries respectively [5].

While burns have a huge impact physically on the individual affected, they also have a large economic impact, accruing costs both in terms of medical treatment and loss of productivity. The Canadian government estimated economic losses of up to 366 million dollars Canadian in 2010 due to burns, 177 million of which are direct costs, while 188 million are from indirect impacts (lost work etc.) [6]. It can therefore be put forward that the expedient healing of burn wounds is important both for the physical and economic health of the individual and the society within which that individual resides. The principles of burn wound healing are similar to that of more commonly encountered wounds that the body is able to deal with relatively easily, but burns have several complications that make the process more difficult. Burns are typically formed with 3 zones, those being, from innermost to outermost, the zones of coagulation, stasis and hyperaemia [4], [7], [8], [9], [10].The zone of coagulation is the main point of the burn wound in which tissue death is inevitable while the zone of stasis surrounding it initially contains tissue that can be saved if the appropriate interventions are carried out. Typically blood vessels have been sealed or destroyed in the zone of coagulation, thus preventing the initial healing processes from

taking place. Over the course of healing, the zone of coagulation will either expand to include the zone of stasis, often due to additional issues such as infection [4], resulting in a more grievous wound; or the tissue can be saved resulting in a healthier outcome and less tissue death. Current methods for detecting infection are laborious and slow to yield results, as they require specimens be analysed in a microbiology laboratory [7], potentially resulting in precious treatment time being lost. Some examples of techniques used to monitor burns for infection include regular surface swabs and tissue biopsies after which the samples are cultured on agar plates for 24 hours before analysis.

Burn wound healing is made up of the three broad phases of inflammation, proliferation and remodeling [9], [10]. The initial phase of inflammation is characterized by the migration of immune system cells, notably neutrophils and monocytes, to the site of injury before other immune system cells such as macrophages, which are either resident in the tissue or produced from monocytes, start to work [9], [10]. During the inflammatory phase the immune system cells previously mentioned are responsible for preventing infection, clearing dead tissue and releasing signalling molecules, like for example growth factors [9], [10]. Activated and attracted by the chemical signals released by the immune system cells, fibroblasts begin migrating into the wound area, in order to start the next phase of burn wound healing, proliferation [9]–[11]. The main purpose of the proliferation phase is to begin closing the wound and rebuilding tissues such as blood vessels [9], [10]. During the final phase of remodeling, the extracellular matrix laid out in the proliferative phase is modified and added to with more collagen and elastin being laid down [9], [10].

Of course the healing process just outlined is in a relatively ideal situation and often infection is a large concern due to the now heavily compromised immune system. The

immune system of burn patients is compromised in several ways, the first being broken skin and the second, only in cases of extreme burns, compromised immune system cells. The skin is a large part of the innate immune system, serving as an effective barrier to all of the bacteria and other microorganisms we encounter in our daily lives [10]. Immune system cells can be compromised in an increasing inflammatory cycle known as "systemic inflammatory response syndrome" [9], wherein the unrestrained release of cytokines and chemokines (largely by immune system cells) leads to the repression of integral parts of the immune system such as neutrophil action to kill invading bacterium [9]. Of the infectious microorganisms commonly found in burns one in particular stands out.

1.2 Burn Infection

Due to the often severely compromised immune system of burn patients they are ripe targets for infection by opportunistic bacteria. One of the most prolific [7] and deadly bacterial species when it comes to infections found in burn wounds, is *Pseudomonas aeruginosa*. *P. aeruginosa* is a rod-shaped, Gram-negative, aerobic bacteria, that is commonly found in soil and water samples [12] and is a normal part of the skin biome. While not normally an issue for healthy individuals, *P. aeruginosa* attacks immune-compromised members of society, such as those suffering from major burns [12]. A huge problem in the modern health care setting, especially in burn wards, *P. aeruginosa* infections have had in some cases up to a 77% [13], [14] mortality rate (when looking at those patients infected with this bacteria). With 127,000 [2] burns reported per year within Canada alone and reports of up to 9% [14] of patients in burn wards developing infections as shown in one 25 year review of a single burn center, burn infections are a major problem. More so than many of the other bacteria commonly found

in burn wounds, *P. aeruginosa* is a particularly nasty culprit, often leading to mortality or increased rates and lengths of morbidity [15]. It has been shown that *P. aeruginosa* is capable of growing in burn wound exudate and that the bacteria's virulence is even enhanced under such conditions [15]. In part due to the risk of infection, treatment of burn wounds can be excruciatingly painful for patients. The World Health Organization (WHO) recommends dressing changes up to twice daily to prevent oozing through the dressing and to check for infection [16].

One of the problems with *P. aeruginosa* is its tendency to produce virulence factors that aid the bacteria to survive and cause serious damage to the infected host. One of the virulence factors produced only by *P. aeruginosa* is pyocyanin, a blue-green, redox active, phenazine [17], [18], that is capable of killing Neutrophils [19]–[21]. Some of the specific effects of pyocyanin on cells exposed to it include effects on cellular respiration [18], [22], [23], modification of immune system functions [18], [22], [24], modification/impairment of enzyme actions [18], [22], [23], as well as general cytotoxicity due to oxidative stress from the production of superoxide and hydrogen peroxide [22], [25]. The chemical structure of pyocyanin is shown below in Figure 1 reprinted from Hall et al. [25].

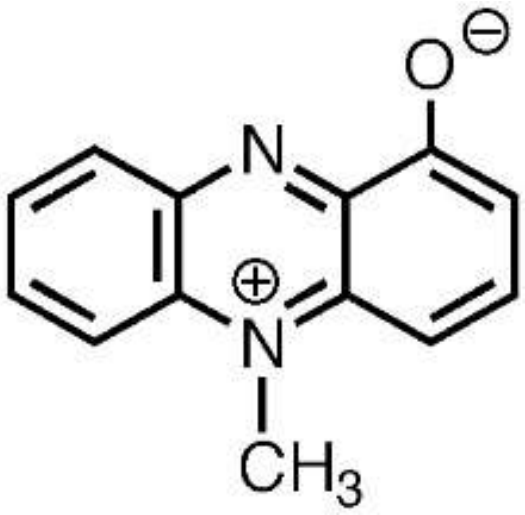

Figure 1: Chemical structure of pyocyanin. Reprinted with open access permission from Hall et al. [25] Creative Commons Attribution License.

There are two positive aspects to the production of pyocyanin, the first being that due to its redox active nature, the virulence factor can be detected through the use of non-functionalized electrochemical sensors and that secondly it is a virulence factor produced uniquely by *P. aeruginosa* [26] and can therefore be used as a specific biomarker for the bacteria. Standard procedures for identifying bacterial infections still involves the use of culture techniques that can take anywhere from 24 to 48 hours [26], creating a need for fast reliable detection potentially through the electrochemical avenue presented by pyocyanin. The prompt, in situ detection of *P. aeruginosa* infections has the potential to go a long way in improving burn patient outcomes.

1.3 How Pyocyanin is Made and What it Does

The synthesis of pyocyanin, a chemical introduced in the previous section, is an important biological function of *P. aeruginosa* and biofilms constructed by strains deficient in its production have been shown to have difficulty forming biofilms (more on biofilms shortly). Pyocyanin production is positively regulated by quorum sensing via quinolone molecules [18], this is due to the fact that it is only worthwhile producing virulence factors

such as pyocyanin for the bacteria if others are doing the same. Essentially it ensures that there will be a sufficient concentration of pyocyanin to be effective before the individual cells commit to producing it, meaning in turn that the more bacteria is present the more pyocyanin will be produced. As a brief aside, quorum sensing is a method by which bacteria and other microorganisms self-organize. In this case bacteria continuously release chemical signalling molecules, meaning that the more cells there are present the higher the concentration of the signalling molecules will be. In our example of *P. aeruginosa* a high concentration of one of these signalling molecules is necessary before the genes responsible for pyocyanin synthesis are expressed.

The main precursor of pyocyanin is two molecules of chorismic acid which are used by enzymes encoded by phz operons (can be thought of as the functional unit of bacterial genes) [27] to produce Phenazine-1-carboxylic acid (PCA) [18], [26]–[29]. PCA is actually the precursor for a variety of phenazine compounds each with their own synthesis pathways, utilizing different Phz proteins [26], [27], [29]. As seen in the Figure 2 below from [39] the PhzM and PhzS proteins are necessary for the transformation of PCA to pyocyanin. PhzM is thought to closely resemble in form and function an O-methyltransferases (enzymes that attach methyl [CH3] groups to molecules, as can be seen by the replacement of the hydrogen atom attached to the lower nitrogen in the middle ring with a CH3 group, in Figure 2 [26] below) similar to those found in other bacterial species [27], [29]. PhzS is thought to be similar in nature to a hydroxylases [29] (which are enzymes that add hydroxyl groups to compounds).

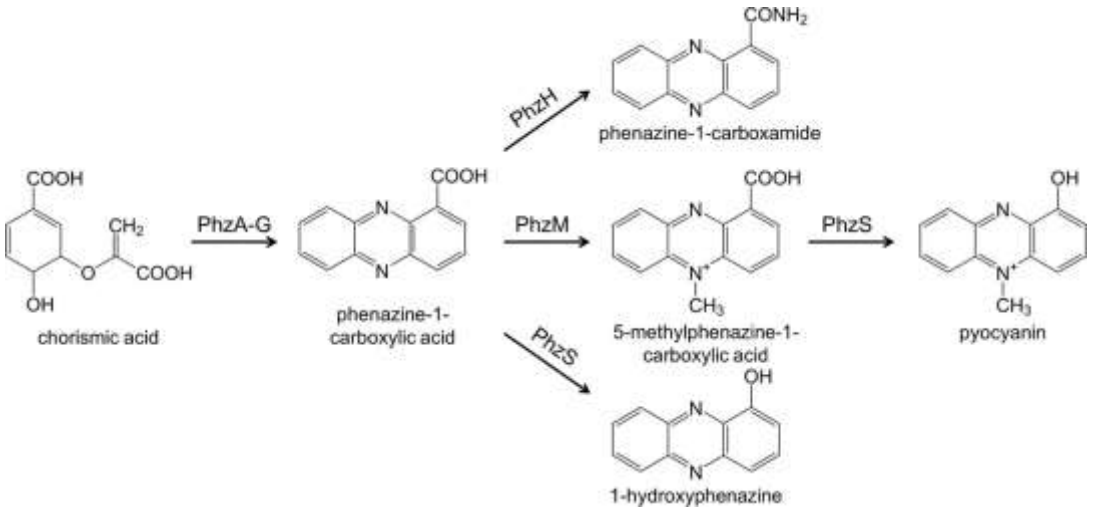

Figure 2: The biosynthesis pathway from chorismic acid through to pyocyanin, using the PhzM and PhzS enzymes. Reprinted with permission from Sismaet et al. [26] Elsevier.

As briefly touched on in the previous section pyocyanin can have a number of negative consequences for the host, once the toxin has been released by the bacteria. One of the mechanisms through which pyocyanin negatively affects eukaryotic cells is redox cycling near or inside the mitochondria (the site of cellular respiration – which is the synthesis of adenosine-tri-phosphate, the main energy currency of the cell) [23]. The redox cycling of pyocyanin in eukaryotic cells is shown below in Figure 3 from Hall et al. [25] and shows how pyocyanin is reduced by nicotinamide adenine dinucleotide phosphate (NADPH, a cofactor) before subsequently transferring its newly acquired electron to oxygen forming superoxide and then possibly hydrogen peroxide.

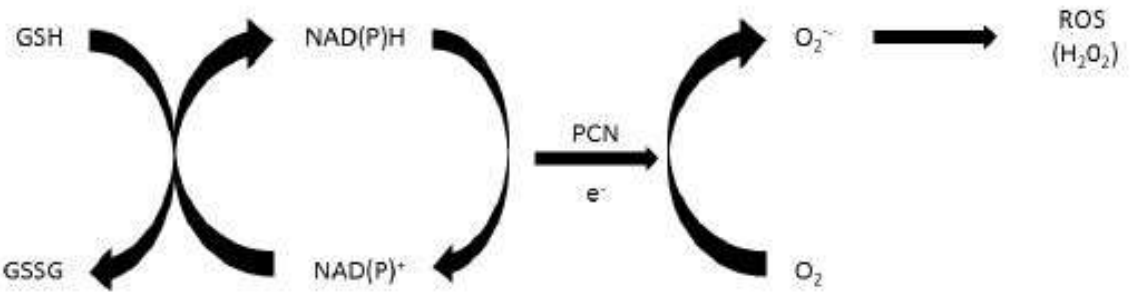

Figure 3: Redox cycling of pyocyanin in eukaryotic cells, thanks to its reduction by NAD(P)H and subsequent electron transfer to oxygen. Reprinted with open access permission from Hall et al. [25] Creative Commons Attribution License.

1.4 How is Pyocyanin Detected Electrochemically?

Due to the redox active nature of pyocyanin it is a prime candidate for detection and analysis through the use of electrochemical techniques. A common electrochemical technique called square-wave-voltammetry is commonly used to reduce and oxidize pyocyanin. Square-Wave-Voltammetry (SWV) involves the use of a potentiostat to maintain precise voltage levels between a carbon working electrode and a silver chloride reference electrode while current is supplied to the system through the counter electrode. The purpose behind having the third reference electrode to maintain voltage is that as the current flows through the counter electrode it would be very difficult to maintain a voltage based on Ohm's law, as can be seen in equation 1 below, the voltage is directly dependant on the current. If the voltage is constantly changing due to the supplied current it would be next to impossible to accurately control the voltage and produce the waveforms necessary for the technique.

$$V = I * R \tag{1}$$

The need for a precise reading of voltage, as can be seen in Figure 4, is due to the complex waveform used in square-wave-voltammetry, a square wave and staircase function combined.

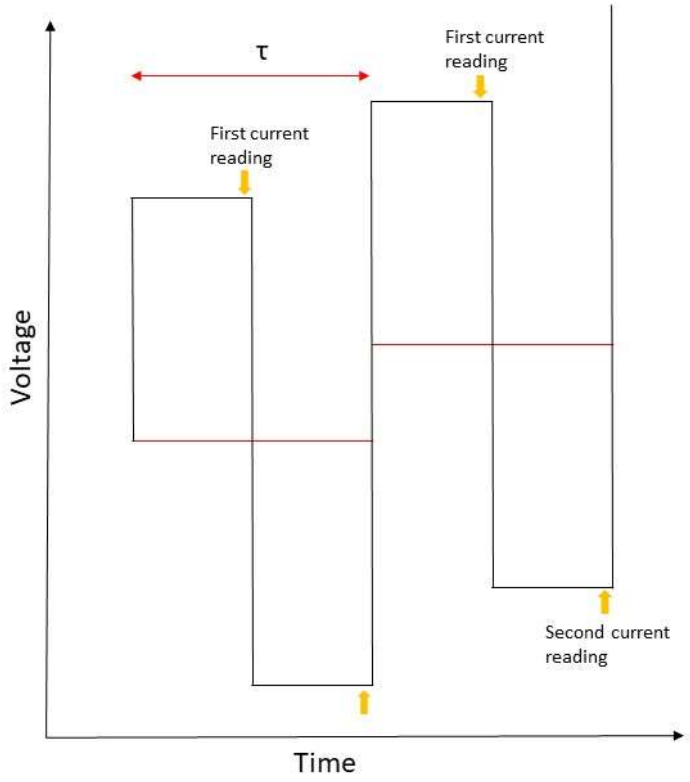

Figure 4: Voltage waveform for Square Wave Voltammetry. Two current readings are taken in every voltage cycle, one at the end of the forward pulse and one at the end of the negative pulse. The voltage period is denoted in red, while the time of current readings are marked by yellow arrows.

The current flowing into the working electrode is sampled twice during each cycle, before they are subtracted from each other, eliminating the capacitive/charging current (essentially the stream of electrons fed into the system by the counter electrode) in the process. Left behind is the faradaic current, which is due to electron transfer at the working electrode surface due to the redox cycling of the chemical species under investigation (the chemical of interest will oxidize and reduce in concert with the forward and reverse voltage pulses) (the surface area of the electrode exposed to the solution is therefore an important variable

when taking measurements). Different chemicals are susceptible to this voltage induced redox cycling at different voltages (different environmental conditions) allowing for the detection of a variety of substances.

1.5 Biofilm Formation

Biofilms can be thought of as one of the most abundant environments life makes for itself. While biofilms themselves are not living things, they are inhabited by a multitude of microorganisms, some of whom make biofilms and some of whom simply inhabit those made by others. Biofilms are found everywhere from creeks in the forest, to medical equipment in hospitals and can be inhabited by a multitude of species or one singular species. Unfortunately biofilms can also become established in burn wounds, rendering infections far more difficult to treat. The end goal of biofilms is the protection and success of their inhabitants [30]. These complex heterogeneous structures are not static in time and change and evolve in response to external stimuli in order to better suit the needs of their inhabitants [30]. Biofilms are composed of both living cells and organic support material known as extracellular polymeric substances (EPS). The EPS is produced by the cells that inhabit the biofilm with different organisms producing different materials. Despite this variety, the composition of the EPS can be broken down into the following general categories: polysaccharides, proteins, DNA/RNA and fats [30]–[33]. Cellular structures such as pili, fimbriae and flagella play roles in maintaining the structure of biofilm and in the attachment of cells to the biofilm and substrate surface [30], [31], [33]. The structures of biofilms and the phenotypes displayed by the cells that inhabit them vary greatly based on a number of variables, such as the species of bacteria present, the strains of said bacteria, the amount of bacteria present and environmental conditions (such as heat, shear forces

due to fluid flow and nutritional elements that are available) [31], [33]. This variety of biofilms is also displayed by the species of bacteria of interest in this thesis, *P. aeruginosa*. *P. aeruginosa* biofilms are a major issue in the health care setting, causing infections in the lungs and airways of cystic fibrosis patients, implantable medical devices, chronic wounds and burn patients [34], [35]. Despite the variations in make up most *P. aeruginosa* biofilms and those of other bacteria go through a predictable 5 step lifecycle. The steps of the *P. aeruginosa* biofilm lifecycle are the initiation of attachment by planktonic (cells free in media) bacterial cells to a surface (at this stage still reversible), the formation of micro colonies and irreversible attachment to the surface, proliferation and the initial production of EPS, maturation into fully 3D structures (often shaped like mushrooms, with a cap and shaft [36]) in which nutrients, oxygen and cells can move and finally dispersion into the environment in order to find new locations to set up shop [33], [34], [37], [38]. Figure 5 below taken from Olivares et al. [37] shows the lifecycle of biofilms graphically.

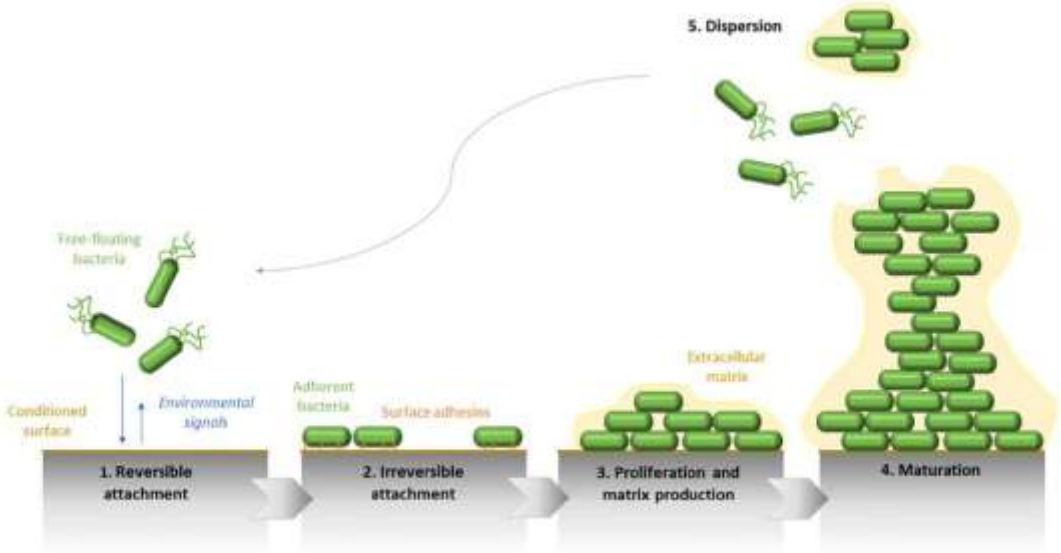

Figure 5: Five stages of *P. aeruginosa* biofilm development. The first stage is reversible attachment, the second is irreversible attachment, the third is proliferation and matrix production, the fourth is maturation and the fifth and final phase is dispersion into the environment. Reprinted with open access permission from Olivares et al. [37].

Biofilms are a large part of the problem of infected burns because they make the bacterial infections far more resilient. In particular bacteria become more resistant to antibiotics, the principle treatment option for wound infections. It has been theorized that this increased antimicrobial resistance is due to several major factors, namely delayed and diminished antibiotic delivery due to the biofilm environment and material components as well as the lowered growth and activity rates of bacteria deeper in the biofilm [39], [40]. Suci et al. [39] performed an in-depth investigation of ciprofloxacin penetration into *P. aeruginosa* biofilms and found that there was a significant reduction in the amount of ciprofloxacin that diffused through the biofilm structure. The lowered diffusion and activity of antibiotics in biofilms is likely due to difficulty of the antibiotic molecules physically diffusing through the biofilm material as well as due to interactions with the variety of materials found in biofilms that can either chemically modify the antibiotic or in a sense grab onto it, slowing its diffusion [40]. The principle behind the lowered growth rate hypothesis is that deep within the biofilm there are fewer nutrients and less oxygen. This starved environment induces the bacteria to have a slower metabolism therefore up taking less of any antibiotic that diffuses down into the lower reaches of the biofilm [40] it also slows down cell division which affects the efficacy of the drug.

1.6 Treating *P. aeruginosa* Infections

Once detected a common choice of tool for combatting *P. aeruginosa* infections is an antibiotic called ciprofloxacin. ciprofloxacin is a fluorinated quinolone that affects most gram-negative and many gram-positive bacterial species [41]. ciprofloxacin is the first choice among quinolone antibiotics when it comes to the treatment of *P. aeruginosa* [42]. Like other quinolones ciprofloxacin targets DNA gyrase and topoisomerase 4 [41]–[43].

Both DNA gyrase and topoisomerase 4 are involved in the coiling and uncoiling of bacterial DNA during the replication process [43]–[45]. Figure 6 below from [45] shows the roles of DNA gyrase and topoisomerase 4 in DNA replication; topoisomerases most prominent role is unlinking interlinked chromosomes right before cell division.

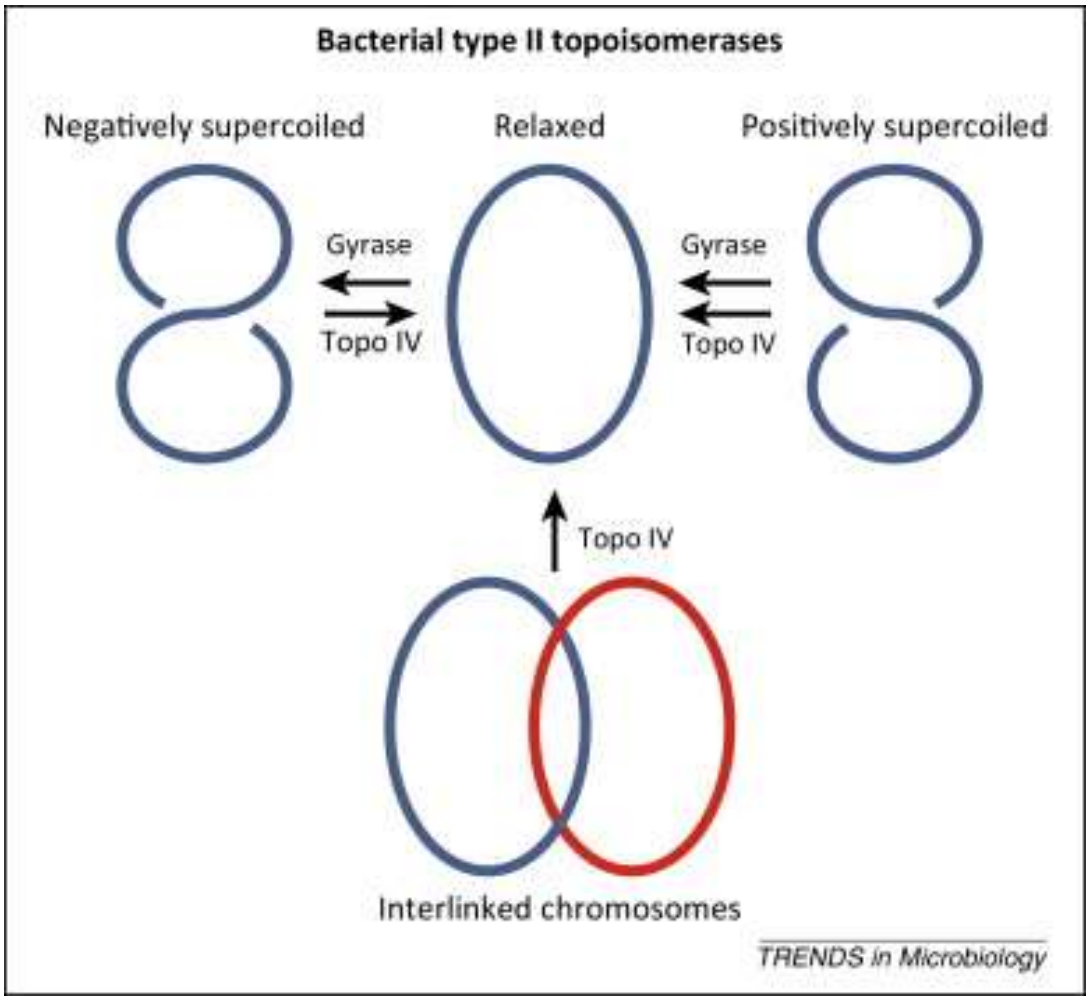

Figure 6: Role of bacterial type 2 topoisomerases. Reprinted with permission from [45]

Both of these enzymes are composed of 2 subunits, one involved in splitting DNA coiling and the other in energy transduction from the hydrolysis of adenosine triphosphate (ATP) (to allow for the DNA splitting and joining/coiling) [42], [45]. In order to perform their roles the aforementioned enzymes have to covalently bond to the DNA strands [45]. Once this has occurred the enzyme-DNA complex is vulnerable to ciprofloxacin which

irreversibly binds to the complex, sealing them together and breaking up the DNA [42], [45].

While antibiotics have proven to be effective against motile bacteria, they have much more difficulty clearing infections that have formed biofilms. As was discussed earlier several EPS components are known to bind aminoglycosides another type of antibiotic commonly used to treat bacterial infections. Suci et al. [39] showed that some regions of biofilms environment experienced 30 to 70 percent less ciprofloxacin than the bulk media concentration through which it was delivered. It has been postulated that this is due to multiple factors such as entrapment or modification by the EPS [39] (modification likely due to extracellular enzymes). It has also been theorized that increased survival of bacteria in biofilms exposed to antibiotics such as ciprofloxacin is due to the antibiotic arrival being slowed and spread out enough for bacteria to produce resistance factors [39].

1.7 Previous Attempts to Detect *P. aeruginosa* Electrochemically

Sharp et al. [46] demonstrated the electrochemical detection and analysis of pyocyanin at clinically relevant concentrations using a carbon fiber electrode and a μAutolab type 3 potentiostat (Eco-Chemie, Utrecht, Netherlands). Physiologically relevant concentrations of pyocyanin were detected, ranging from 1 – 100μM. The sensor is comprised of roughly 2000 fibers, 10μm in diameter sandwiched between two pieces of laminated plastic before the fiber array was baked with an unidentified resin to form one large sensor. The intra batch stability of the sensors was investigated with strong consistent signal strength found across multiple batches of electrodes. The length of the sensors are not included in the paper, however a rough estimate for the diameter at 20mm can be calculated based on the fiber diameter. The sensors are therefore likely small and could

potentially be attached to the surface of a wound dressing, but not easily integrated inside of one. Webster et al. [21] used commercially available disposable electrode arrays and square-wave-voltammetry (the principle method used to detect pyocyanin electrochemically), to both detect clinically relevant concentrations of pyocyanin (once again 1-100μM) in spiked human fluid samples and to demonstrate that several other species of common bacteria do not produce anything that would interfere with the detection of pyocyanin via SWV. It was shown that two different strains of *Escherichia coli, Staphylococcus aureus, Staphylococcus epidermidis* and *Bacillus cereus* produced no factors with similar peaks when undergoing square wave voltammetry from -0.5 to 0.0 volts. The limit of detection for pyocyanin in a variety of human bio fluids were determined such as 1.81μM for urine and 0.16μM for blood-heparin. The potentiostat used in this study was the CHI 842C, costing $9500 [47]. Sismaet et el. [26] used the same disposable electrodes as Webster et al. [21] and a CHI 1040C potentiostat to investigate pyocyanin production in clinical samples from 94 patients, all of which demonstrated pyocyanin production. Sismaet et al. [26] also showed through genomic analysis that 99.9% of the known *P. aeruginosa* strains had the two genes (PhzM and PhzS) necessary for pyocyanin production; lending credence to the idea of using this phenazine compound as a biomarker for *P. aeruginosa*. Ciui et al.[48] utilized similar printed electrodes on nitrile gloves coupled with an Autolab PGSTAT 302N potentiostat to detect pyocyanin and pyoverdine, both virulence factors of *P. aeruginosa*, on various surfaces and while contaminated with a variety of disinfectants likely to be found in a hospital setting. While many of the aforementioned studies successfully detected pyocyanin, none of them did so with both inexpensive and flexible electrodes as well as affordable and portable potentiostats.

1.8 Smart Bandages

Detecting chemical markers is a good first step, however interest in smart bandages and wearable health monitoring technology that brings analytical ability to the point of care has been on the rise for some time now [49], [50]. Applications for wearable, sensing technology, including smart bandages, have been found in the detection of harmful agents [51], detection of the biomarkers of infectious agents [48], chronic wound monitoring and treatment [52], [53] as well as determining users physiological state through the electrochemical analysis body fluids [54], [55]. Mishra et al. [51] developed a system whereby electrodes printed onto a nitrile glove were coupled with a miniaturized, wearable potentiostat (EmStat3 blue, Palmsens) coasting roughly $3000, in order to detect dangerous organophosphate compounds on different surfaces. The work done by Mishra et al. [51] is similar to that carried out by Ciui et al. [48] but shows how a portable potentiostat system could be used to detect *P. aeruginosa*. Both Mostafalu et al. [52] and Mirani et al. [53] developed pH sensing hydrogel wound dressings to detect and treat bacterial infections in wounds. Mostafalu et al. [52] took a more involved route with the use of PANI coated pH sensors, screen printed on paper, that were developed by Rahimi et al. [56]. A microcontroller served as the brains of the system by monitoring the sensor array and triggering antibiotic release, via a heating array and thermo responsive micro particles, once a suitable pH change was detected. Mostafalu's work demonstrates the possibility of a self-contained wound monitoring system, but makes use of sensors monitoring for general symptoms of infection not bacteria specific markers. Mirani et al. [53] took a more passive approach and utilized chemical pH indicators to detect pH changes brought on by bacteria. Brilliant yellow and Cabbage juice change color when in different pH solutions

and were infused into beads before being 3D printed into alginate meshes and then encased in the overall alginate dressing. These pH sensitive patches were combined with drug eluting scaffolds made in a similar fashion. Lastly Mostafalu et al. [55] developed a suite of thread sensors for the detection of physiological parameters, that are easily integrated into existing wound dressings; while sensors weren't developed for the specific detection of pyocyanin and subsequently *P. aeruginosa*, glucose sensors were coupled with a custom made potentiostat board. While the previously described work set up a great ground work, potentially enabling healthcare practitioners to say "yes there is an infection", it does not help to identify the specific microorganism causing the infection, leading to a continued dependence on laboratory analyses for final determination of the insulting species.

1.9 Current Work

Despite the remarkable advances previously outlined, to date, there are no systems that combine the detection of bacterial infections through specific biomarkers, with the delivery of the right therapeutics for the job, in one affordable and portable package. Herein we report a system that combines specific bacterial detection and treatment. Low-cost sensor and drug eluting threads were developed using a simple layering technique with the help of a squeegee and casting (for the drug releasing threads) methods. The sensors are coupled with a low-cost, portable, open source potentiostat described by Ainla et al. [57]. The sensors were rigorously tested both for the detection of pyocyanin over a spectrum of physiologically relevant concentrations as well as their susceptibility to interference from other materials and finally their biocompatibility. Meanwhile effective control of drug release, was established; an important factor given the rise of antibiotic resistant bacteria.

As seen in Figure 7 below the system consists of 4 subsystems, those being the three pyocyanin detecting non-functionalized electrode threads as well as the drug releasing hydrogel encapsulated heating element threads, the microcontroller controlled, wearable, open source potentiostat and finally a smartphone for wireless communication, control and instantaneous data readout. With these subsystems combined, burn wounds can be effectively monitored and managed for infection by the *P. aeruginosa* pathogen.

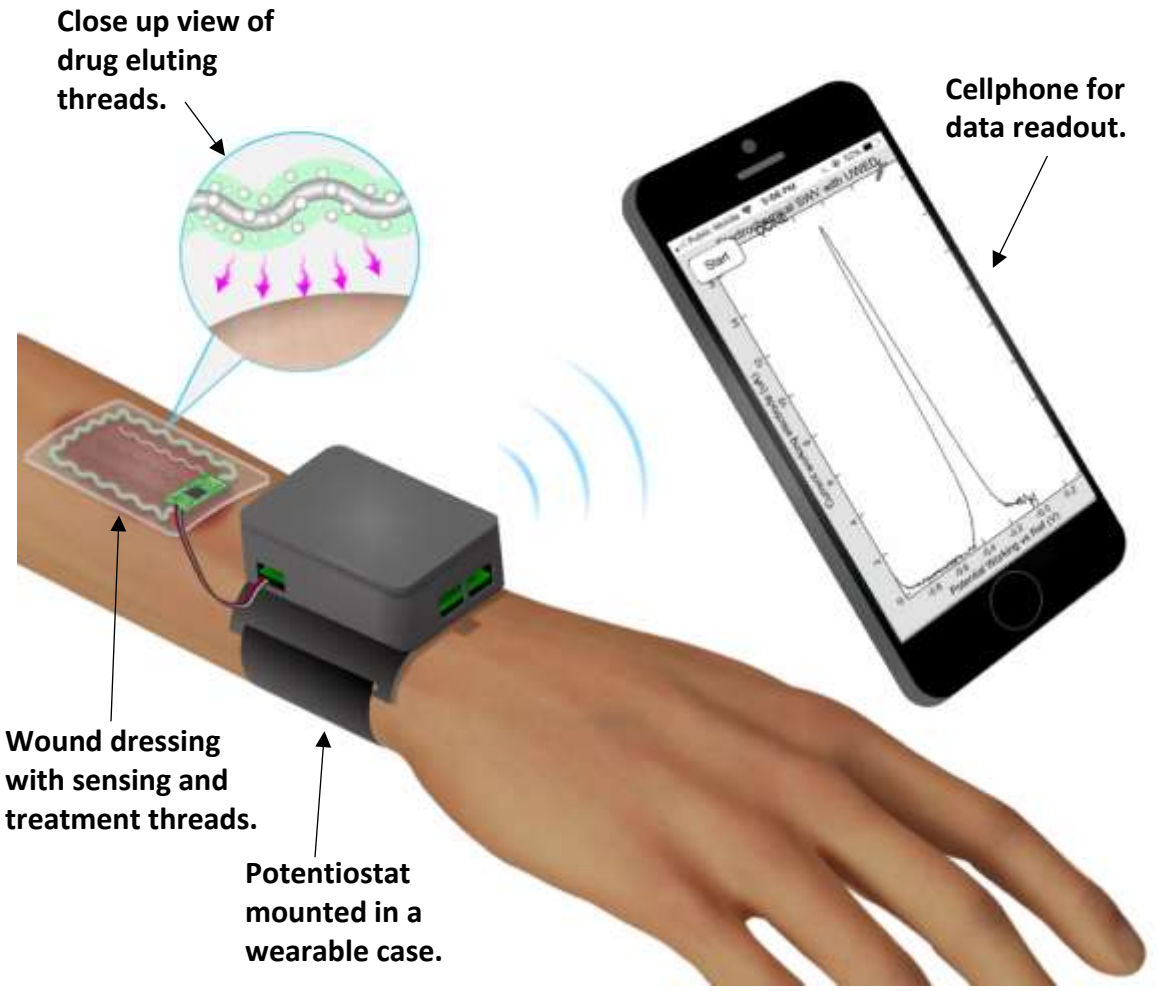

Figure 7: Schematic of the proposed system. A) A cellphone used to control the potentiostat and display the results of electrochemical tests. B) The potentiostat mounted in a wearable case for attachment to a patient. C) Medical dressing with three sensing threads as well as one drug eluting thread woven within. D) Close up view of the drug eluting thread, coated in alginate intermixed with PNIPAM-PEGDA particles.

Pyocyanin being a specific biomarker for *P. aeruginosa* [26] and being redox active makes for an excellent candidate for the electrochemical detection and identification of *P. aeruginosa*. Using thread based technology to detect the pyocyanin biomarker has several advantages in that it is inexpensive and innately flexible; allowing for the thread based technology to be integrated into new and existing wound dressings. Thread based technology can also draw on the long established techniques used by the textile industry to create new patterns and integrate sensors and drug delivery threads into pre-existing fabric patterns. While detection and identification are important aspects of dealing with infections in burn wounds, equally as is important is the timely deliverance of the appropriate therapeutics. Timing is important when it comes to burn management as infections become harder to deal with, the more entrenched they become, establishing biofilms and taking a large toll on the patient. The addition of the on demand drug eluting threads allows for the immediate application of antibiotics, in this case ciprofloxacin, indicated for use with *P. aeruginosa* [42], [58]. Like other quinolones, ciprofloxacin targets DNA gyrase and topoisomerase 4 [41]–[43]. Both DNA gyrase and topoisomerase 4 are involved in the coiling and uncoiling of bacterial DNA during the replication process [43]–[45]. Both of these enzymes are composed of 2 subunits, one involved in splitting DNA coiling and the other in energy transduction from the hydrolysis of ATP (to allow for the DNA splitting and joining/coiling) [42], [45]. In order to perform their roles the aforementioned enzymes have to covalently bond to the DNA strands [45]. Once this has occurred the enzyme-DNA complex is vulnerable to ciprofloxacin which irreversibly binds to the complex, sealing them together and breaking up the DNA [42], [45].

While thread based electronics are inexpensive and easily integrated into existing wound treatment programs, the electronics associated with using the electrodes are normally expensive and bulky. Potentiostats are necessary to run square-wave-voltammetry on a three electrode system, however potentiostats can cost tens of thousands of dollars, with even the small portable commercial versions costing in the thousands of dollars range. An inexpensive, wearable and open source potentiostat designed by Ainla et al. [57] is utilized in this work, demonstrating that there are affordable alternatives for electrochemical analysis in a healthcare setting. With results shown to be similar to those of commercially available options, the open-source potentiostat is a fraction of the cost at under a hundred dollars.

Prior studies have for the most part focused on either just detecting specific biomarkers or when also treating infections detecting them through general non-species specific indicators. The overall goal of developing the components of an affordable and wearable smart wound dressing that can detect and treat a specific infection, in this case *P. aeruginosa*, in clinical burn wards has been met.

Chapter 2: Thread Based Electrodes

2.1 Why Cotton Threads?

There has been growing interest in affordable, point of care diagnostic systems for some time, as they offer quick turnaround times for analyses and cut out the middle man, in this case laboratories [59], [60]. There has also been growing interest in utilizing everyday materials such as cotton threads to fulfill this role. Mostafalu et al. [55] developed a suite of thread based sensors for medical diagnostics, showing how inexpensive, flexible materials can be used in medical diagnosis. The flexibility, low cost, accessibility and ease of manufacturing are some of the major benefits that come with developing sensors out of cotton threads.

2.2 Thread Manufacturing

A variety of threads are manufactured and utilized for this project. The threads can be divided into two sub categories, those utilized in the detection of pyocyanin and those used to carry and release antibiotics. Both subcategories of thread were produced in a similar fashion. Cotton thread was cut into appropriate lengths, with several strands having their ends taped in-between two pieces of double sided tape. The threads were then treated with a plasma machine (DYNE-A-MITE 3D treater, from ENERCON), on each side (flipping the taped ends and hence the threads). Plasma treating was done in order to remove any wax coatings that might have prevented absorption of the conductive inks or wicking of analyte. The threads were then cut from the tape and passed through the tip of a 200 μL pipette tip. The pipette tip was then passed through a squeegee containing silver ink. The squeegees were developed by Karperien et al. [61] and made by cutting a syringe

in half and removing its outlet nozzle before filling the remains of said nozzle with polydimethylsiloxane (PDMS). A small hole was then punched through the PDMS with a 23 gauge needle and the container (remains of the syringes body) were filled with conductive ink. The squeegees were utilized to ensure a more even coating of ink was applied with each pass. Working and counter electrodes were made with three base coats of silver and 3 outer coats of stretchable carbon ink. After each coating with silver ink the threads were suspended horizontally just above a hotplate at 120˚C for 5 minutes before being laid out on the hot plate, still at 120˚C, for a further 10 minutes. The coating process was repeated a further three times with stretchable carbon ink at 120˚C once again. After coating, the threads were cut into the desired length (in this case 3cm), after which dupont pins had their connectors painted in stretchable carbon ink before one end of the thread was crimped in place and the whole assembly was baked at 120˚C for 10 more minutes. A similar process was carried out for reference electrodes and drug eluting electrodes but with only silver chloride ink and straight silver ink being applied during any part of assembly respectively. Lastly the drug eluting threads were cast into a solution of alginate containing the thermo-responsive PNIPAM-PEGDA micro particles, which contained ciprofloxacin.

2.3 Cotton Thread Electrodes Close Up

Shown below in Figure 8 are Scanning Electron Microscopy (SEM) images of the thread based electrodes. The extra base layers of silver on the working and counter electrodes helps with conductivity, and therefore a clearer signal, due in part to its material properties as well as filling out the layers leading to less breaks and irregularities in the conductive outer layers of the thread electrode. Comparing the carbon with silver base coat

threads and silver/silver chloride coated threads with the cotton threads, a much smoother and more uniform outer surface can be seen on the electrodes. The smoother outer surface makes the surface area more controllable, which is important for signal reproducibility. The next section will highlight the difference, quantitatively, in terms of the signal generated by carbon working and counter electrodes with and without a silver base coat.

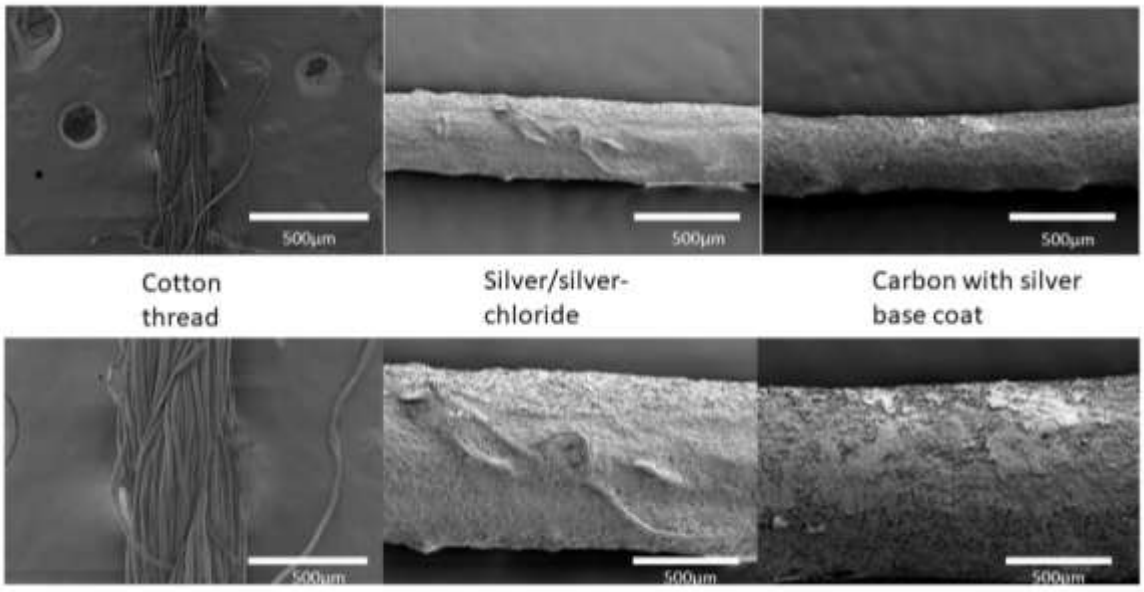

Figure 8: Non-functionalized sensing threads. Notice the smooth uniform surface of the threads coated in conductive material.

Chapter 3: Sensor Characterization

3.1 Detecting Pyocyanin in Ideal Conditions

To demonstrate the system's ability to detect pyocyanin and subsequently the bacteria *P. aeruginosa*, a serial dilution from 1µM - 100µM of pyocyanin was made in PBS, before three biological replicates were measured each with three technical replicate readings taken. To test the sensors 2mL cryotubes were filled with 1.5mL of pyocyanin – PBS solution from the serial dilution. Three holes were drilled in a cyrotube lid, through which the thread sensors could fit. The lid was subsequently glued to a piece of aluminium with a hole cut into it. The same containment vessel lid was used for all the tests, in order to keep the electrode spacing even across replicates. A set of electrode threads plugged into jumper wires attached to the potentiostat would be passed through the lid holes and secured with a grip on the jumper cables. A cryotube filled with the desired concentration could then be screwed in place, thus immersing the threads in the desired analyte. Once a cryotube of pyocyanin was secured 3 readings were taken with the potentiostat using square wave voltammetry with a frequency of 10Hz, a step voltage of 5mV and a pulse amplitude of 10mV. The experimental setup can be observed below in Figure 9. Three rounds of washing with distilled water filled cryotubes was performed between each concentration in an effort to reduce cross-contamination.

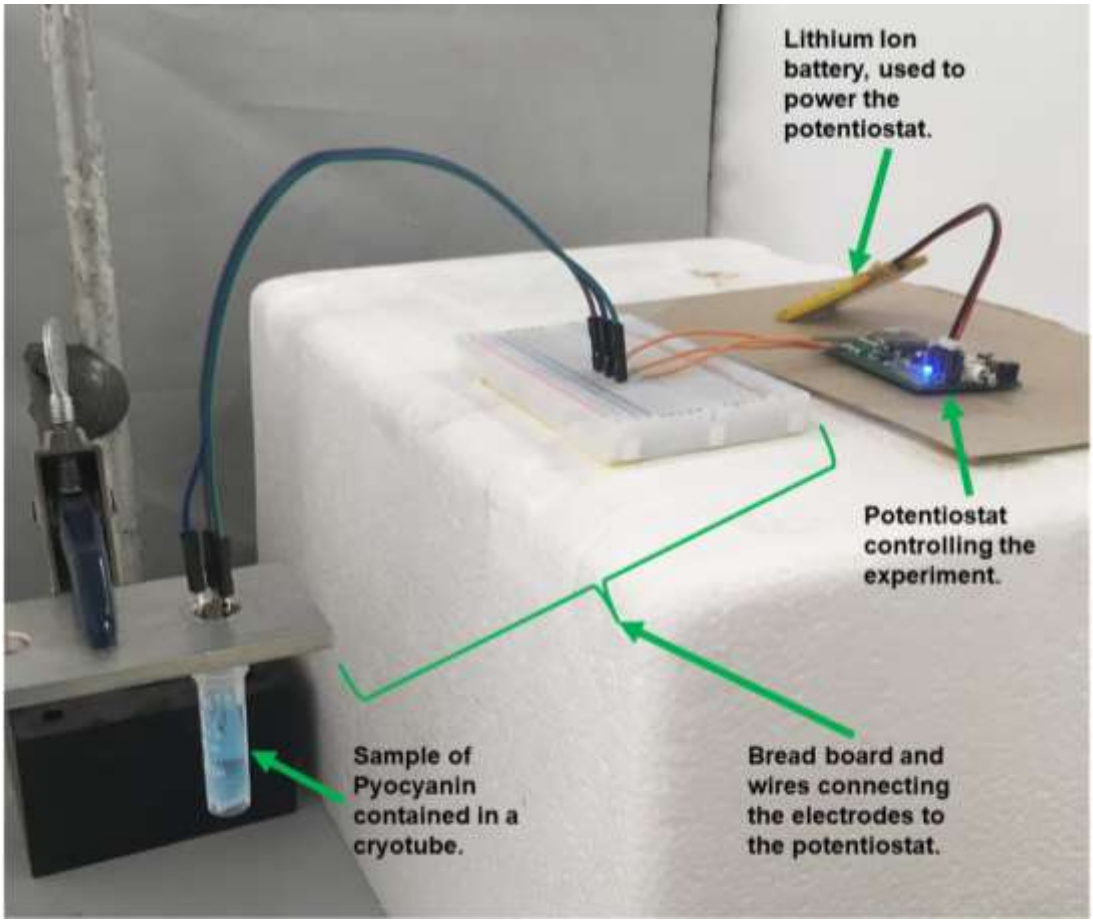

Figure 9: Experimental setup for the characterization of cotton thread based electrodes. A cryotube containing blue pyocyanin is screwed into the holding cap while electrodes are slotted through. The potentiostat circuit board is attached with the electrodes via a breadboard.

As mentioned in the previous chapter the extra silver base layers helped to improve the clarity and linearity of readings for different concentrations of pyocyanin. Figure 10-A and B show a concentration gradient and calibration curve for sets of sensors in which the working and counter electrodes are fabricated with 6 layers of carbon and not silver base layers. The r-squared value is not acceptable at only 0.8012 and the error bars in Figure 10-B (representing the sample standard deviation) show significant overlap.

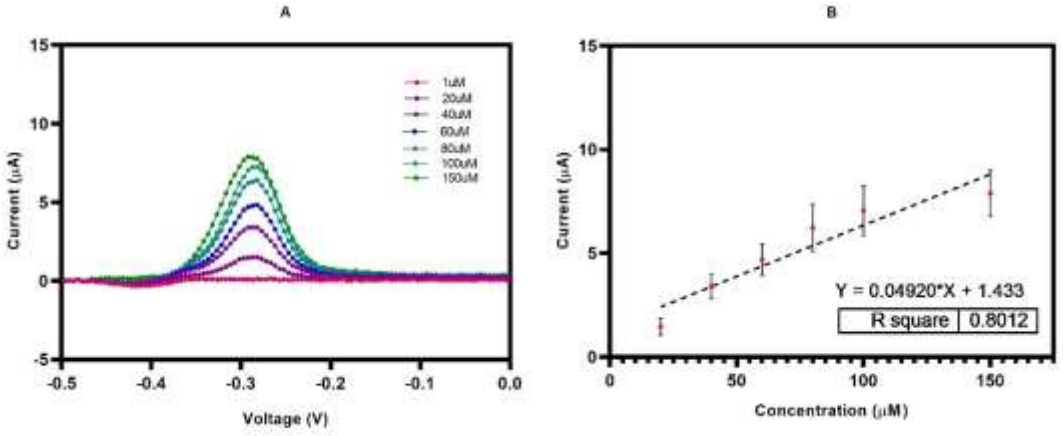

Figure 10: A) The normalized calibration curve for electrodes without a silver base layer, using SWV for concentrations ranging from 1 – 150 µM. B) Standard curve for pyocyanin in PBS using electrodes without a silver base layer, at -0.29V (vs Ag/AgCl). Error bars denote sample standard deviation n=3.

The sensors demonstrated a linear behaviour with an r-squared value of 0.9825, derived from the calibration curve in Figure 11-B. As can be seen Figure 11-A each concentration of pyocyanin is easily distinguishable from the others. Concentrations of up to 130µM have been reported in the sputum of patients suffering from cystic fibrosis [21] while concentrations of up to 25.4µM have been detected in the burn exudate found on soiled dressings of infected patients [62], although the authors noted concentrations were likely higher in the burnt tissue adjacent to the dressings. Findings related to the clinical levels of pyocyanin encountered by healthcare practitioners are within the limits of detection displayed in Figure 11-A.

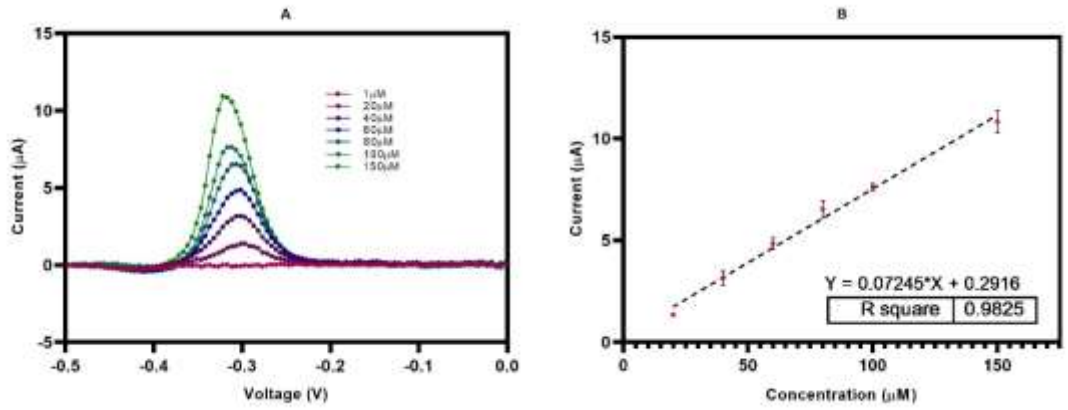

Figure 11: A) The normalized calibration curve for electrodes with a silver base layer using SWV for concentrations ranging from 1 – 150 μM. B) Standard curve for pyocyanin in PBS using electrodes without a silver base layer at -0.29V (vs Ag/AgCl). Error bars denote sample standard deviation with n=3.

The limit of detection for the setup outlined in this thesis was calculated using the process outlined by Armbruster and Pry [63]. First the limit of blank (LoB) was calculated with equation 1 shown below, in which SD stands for standard deviation and the 1.96 is the z value corresponding to a 95% confidence interval.

$$LoB = mean_{control} + 1.96(SD_{control}) \quad (2)$$

Afterwards the limit of detection (LoD) was calculated using equation 2 shown below. The standard deviation associated with 20μM was used in equation 2, as it was the lowest reading distinguishable from the control.

$$LoD = LoB + 1.96(SD_{20\mu M}) \quad (3)$$

Using these formulas a limit of detection for the experimental setup was determined to be roughly 2.4μM.

3.2 Selectivity and Interference Studies

To verify the selectivity of the newly developed thread sensor – potentiostat system, pyocyanin was detected in the presence of a variety of substances likely to be encountered in a medical setting. Some of materials include the cells of the human body itself and their excretions as well as other tools used by health care practitioners to combat infections.

In order to ensure human cells would not interfere with the detection of pyocyanin, HaCat cells (Addexbio, USA, Catalog Number: T0020001) were grown in Dulbecco's modified eagle's medium (DMEM, Gibco™ by ThermoFisher Scientific, Waltham, MA, USA), with 10% fetal bovine serum (Gibco™ by ThermoFisher Scientific, Waltham, MA, USA) and 1% penicillin-streptomycin (Gibco™ by ThermoFisher Scientific, Waltham, MA, USA). The cell media used to grow the HaCat cells as well as some unused media was subsequently spiked with pyocyanin for a final concentration of 75μM of pyocyanin. A similar protocol, as was used for the initial sensor characterization was carried out, with the samples contained in cryotubes for testing. However for this trial technical triplicates were not taken, instead each condition had 3 biological replicates and each replicate had its own set of sensors made for it. As can be seen in Figure 12– A & B there are large differences in the signals from spiked and un-spiked cell media samples, indicating that signal interference from at least the outer layer of skin cells is unlikely. The signals in the presented graphs have not been normalized in order to visually highlight the difference in current produced with and without pyocyanin present in solution.

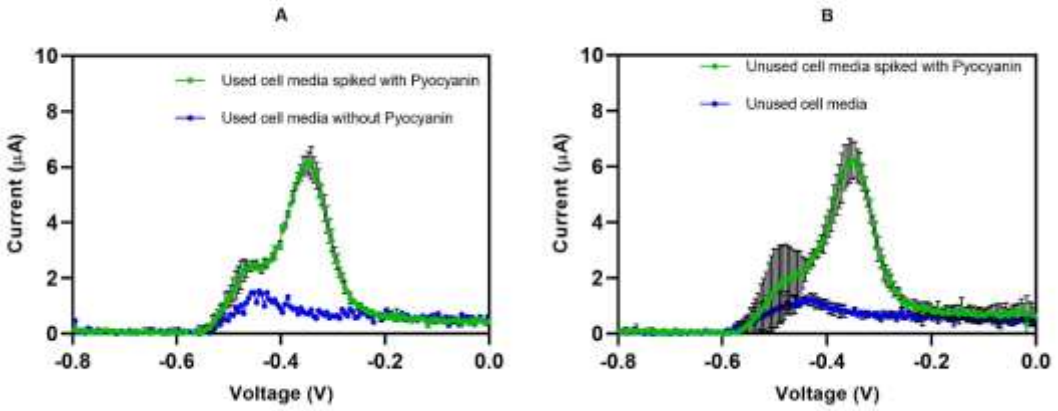

Figure 12: A) Pyocyanin detection in the same solution as unused cell media at a concentration of 75µM. B) Pyocyanin detection in the same solution as cell media used to grow HaCat cells at a concentration of 75µM. Error bars denote sample standard deviation with n = 3.

Human tissue is not the only thing involved in the typical burn healing process, as during the treatment of burns a variety of methods are used in an effort to prevent and treat bacterial infections. It is important that treatment and in particular preventative measures do not interfere with the detection of *P. aeruginosa*; otherwise an infection could be allowed to develop for longer than it otherwise would, with healthcare practitioners trusting incorrectly that the system showed no pyocyanin production. The antibiotic used as the treatment option in the presented system is ciprofloxacin. While antibiotics have been known to hinder the production of pyocyanin, it can be seen in Figure 13 - A that Ciprofloxacin seems to boost the signal generated for the detection of pyocyanin. Interference from Ciprofloxacin was tested for with the same methodology as for possible cell based interferences. The solution was prepared by making an initial 1mg/mL solution of ciprofloxacin in distilled water. Next 0.75mL of the Ciprofloxacin solution and 0.75mL of 150µM pyocyanin in PBS solution were mixed for a final concentration of pyocyanin of 75µM. As seen below in Figure 13 - A the 75µM pyocyanin solution gave off a reading

closer to that which would be expected from a 95-100μM solution or a boost roughly equivalent to an increase in concentration of 20μM. As it turns out ciprofloxacin can be detected electrochemically using both differential pulse voltammetry [64], [65] and Square Wave Voltammetry [66] (the former being closely related to the latter). However the detection peak for ciprofloxacin is all the way up at 1.0 V, far away from the roughly -0.3 V at which point pyocyanin reacts. There have been studies investigating the relationship between ciprofloxacin and pyocyanin; it was shown by Grant et al. [67] that pyocyanin increases the MIC of ciprofloxacin for *P. aeruginosa*. The results attained by Grant et al. indicate the possibility of Ciprofloxacin and pyocyanin interacting; however the authors draw the conclusion that the increased MIC is simply due to changes in the behavior (initiation of biofilm formation) brought on by pyocyanin.

In terms of preventative measures taken against infection the World Health Organization (WHO) recommends the application of either silver nitrate 0.5% aqueous, silver sulfadiazine 1% or 11% mafenide acetate [16]. To date only silver sulfadiazine 1% has been tested, once again following the same methodology as the other signal interference studies. A silver sulfadiazine solution of 1% weight per volume was made in PBS before 1.5mL was sequestered in a cryotube as the control and 0.75mL was added to 0.75mL of 150μM pyocyanin solution to produce a final concentration of 75μM of pyocyanin. The Silver Sulfadiazine solution also raised the peak signal current higher, by a factor equivalent to around 25μM; however another peak wasn't generated where the pyocyanin peak is found as seen, shown in blue, in the control group line in Figure 13 – B. While the presence of both ciprofloxacin and silver sulfadiazine increase the signal of pyocyanin, pyocyanin itself is easily distinguishable from the background signal.

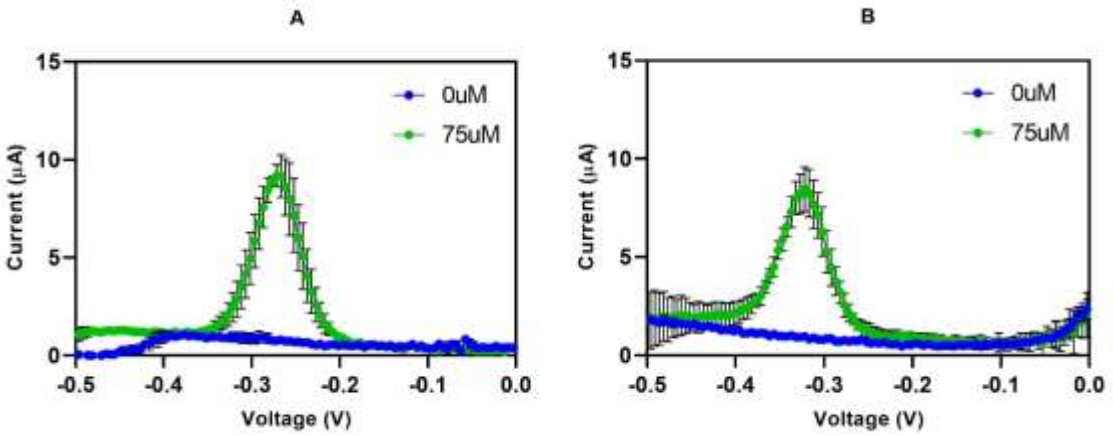

Figure 13: Materials signal interference study. A) Pyocyanin detection in the presence of ciprofloxacin at a concentration of 75µM. B) Pyocyanin detection in the presence of Silver Sulfadiazine at a concentration of 75µM. Error bars denote sample standard deviation with n = 3.

3.3 Stability of Cotton Thread Based Electrochemical Sensors

The ability of the sensors to detect pyocyanin accurately and reliably over time is another important facet of sensor development. One of the benefits of this technology is less of a need to check and change the dressings as often as traditional bandages, however if the sensor signal drifts with time and exposure this would not be a possibility. Stability of the sensors was broken down into three categories, short term stability (on the time scale of minutes and hours), midterm stability (on the time scale of days) and long term stability (on the time scale of weeks and months).

The short term stability of the sensing threads was tested over the course of 24 hours with sensing threads immersed in a PBS solution containing pyocyanin, similar to the original sensor characterization studies. The same solution of 100µM pyocyanin in PBS was used for all the tests. Three different sets of electrodes made up the biological replicates, with each set being left in solution for 24 hour and one reading being taken at 0, 15, 30, 60, 120, 180, 240, 300, 360, and 1440 minutes. As can be seen in *Figure 14* - A the short term signal

stability was well maintained over the course of 24, with a slight dip towards the end of 24 hours. There was no statistical significance between the various different time points. The samples were tested one after another, over the course of a 3 day period, suggesting that the sensors might have at minimum a good 3 day shelf life.

The midterm stability study was carried out in a similar manner with the electrodes being immersed for a week at a time immediately after fabrication. The readings were taken every day at the same time for a week as can be seen in *Figure 14* - B. The signal drifted over the course of the week, resulting in a statistically significant difference between days one and 7, as determined by the one-way ANOVA test using GraphPad Prism version 8 (GraphPad Software, La Jolla, California, USA). The cause of this drop in current is not currently known but could be due to a chemical degradation of the conductive inks.

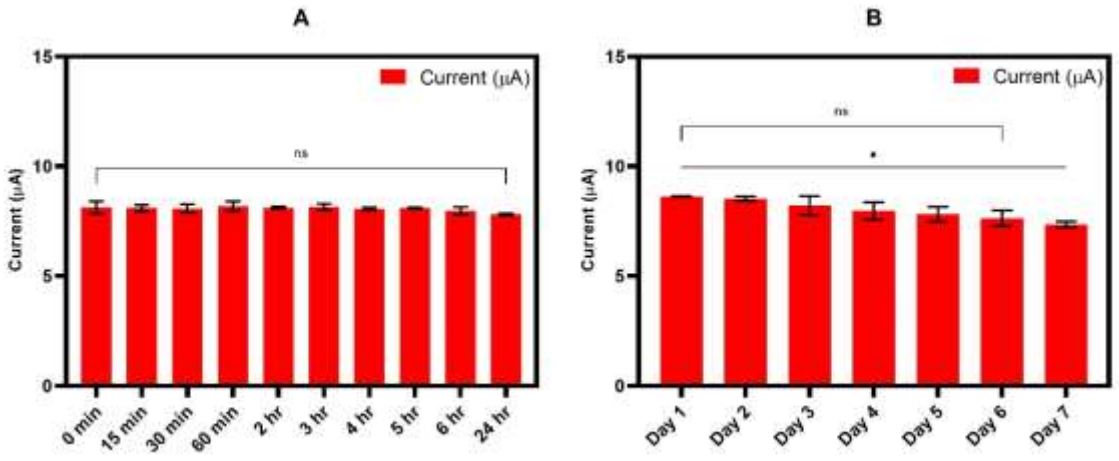

Figure 14: Stability study results. A) Short term signal stability over the course of 24 hours. B) Midterm signal stability study over 3 days. Error bars denote sample standard deviation with n = 3. P-values: *<0.05, **<0.01, ***<0.001, ****<0.0001).

3.4 Real World Simulations of the Thread Sensors in Action

While the principles behind our smart bandage have been proven, it was prudent to test the system in some more realistic settings. The more realistic settings involve the detection of live *P. aeruginosa* on agar plates and the detection of pyocyanin using electrodes that have been woven into a medical gauze.

3.4.1 Materials and Methods

Two plates were used to grow bacteria, while two other plates were not inoculated so as to serve as controls. A *P. aeruginosa* colony was inoculated into 3mL of LB broth and cultured at 37˚C until they had a concentration of 10^8CFU/ml. In the meantime tryptic soy agar (TSA) plates were prepared under sterile condition according to the manufacturer's instructions. 100μL of *P. aeruginosa* infected broth at 10^8CFU/ml was then pipetted onto the agar plates and spread using a cell spreader before further incubation at 37˚C for 24 hours. A blueish green color was observed on the plates. A set of sensors was then placed onto a plate surface and a reading taken in a biosafety cabinet.

A single set of sensors was used for this experiment in order to demonstrate the sensors ability to alternate between contaminated and uncontaminated samples while maintaining the appropriate signal levels. The other bacterial samples were grown using the exact same methodology by culturing the bacteria in broth before being spread over an agar plate and further incubated for 24 hours.

For testing the ability of electrodes to detect pyocyanin after being woven into medical gauze, they were threaded through with the help of a needle. The needle was pressed threw the fabric, after which an electrode was inserted into the needle and the needle subsequently

removed. This was performed for every "stitch". 1ml of 100µM pyocyanin in PBS solution was then placed in a petri dish before the medical gauze was placed within the petri dish as well.

3.4.2 Results and Discussion

Two peaks shown in purple can be observed in Figure 15 – A, indicating different concentrations of pyocyanin produced by the *P. aeruginosa* samples. According to the standard curve developed in PBS this represents a concentration of between 20 - 40µM of pyocyanin, however another standard curve would need to be prepared on agar plates before this value could be confirmed. The purpose of this study was simply to show that a significant difference could be detected between samples with and without *P. aeruginosa*. Figure 15 – B shows the results of using the sensors to detect other bacteria, namely *Staphylococcus aureus, Proteus mirabilis* and *Klebsiella pneumoniae* as well as a control plate of sterile TSA. None of the bacteria exhibited any peaks in current within the measurement window.

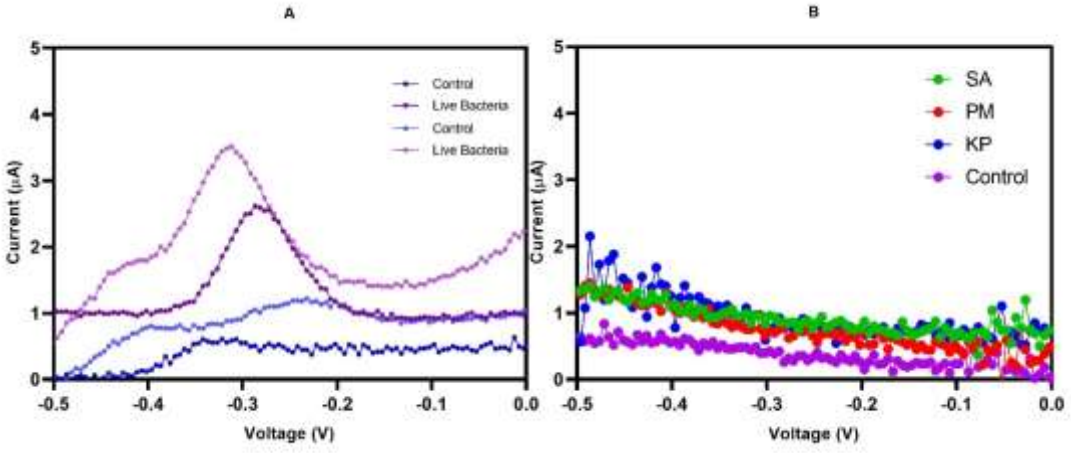

Figure 15: A) Detection of live *P. aeruginosa* bacteria on TSA plates. B) Attempted detection of *Staphylococcus aureus (SA), Proteus mirabilis (PM)* and *Klebsiella pneumoniae (KP)*.

Additionally in order to demonstrate the ability of the threads to be integrated with traditional medical dressings a set of electrodes was woven into some standard medical gauze. The experimental setup and results can be viewed below in Figure 16 A and B. The signal was much lower than for the standard setup when the electrodes are immersed in solution, due to a lot of the pyocyanin being absorbed into the gauze far away from the electrodes; however the results were good enough for a positive identification of *P. aeruginosa*.

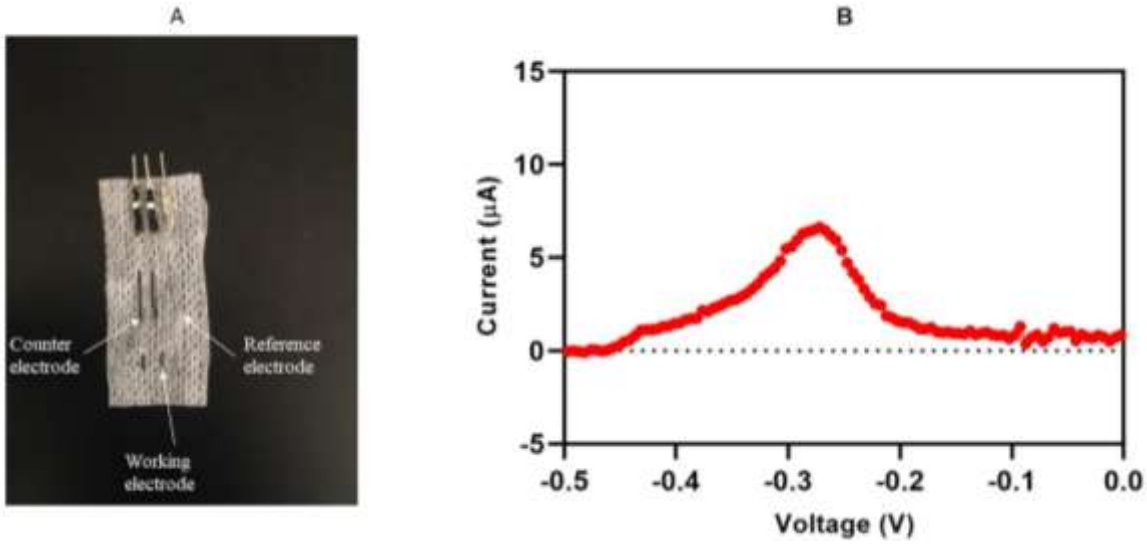

Figure 16: A) Thread electrodes woven into medical gauze. B) Detection of 100uM of pyocyanin with electrodes woven into medical gauze.

Chapter 4: Drug Release Threads

Detecting bacterial infections is important but once an infection has been identified it must be treated as quickly as possible. The sooner an infection is stopped the better. Due to the need to tackle bacterial infections without delay our smart bandage has an integrated drug delivery system. If a positive result is found for a *P. aeruginosa* infection, the user, most likely a nurse, will be notified on their phone or similar interface device. In theory once notified of an infection the health care provider will be given the option to deliver ciprofloxacin to the wound immediately by increasing the temperature of the silver drug eluting electrodes.

The drug delivery system is composed of a cotton thread, coated in several layers of silver. The silver coated thread is in turn coated in 2% (w/v) alginate cross-linked with 1% calcium chloride infused agarose and subsequently 2% (w/v) calcium chloride solution. Within the alginate are suspended thermo-responsive PNIPAM-PEGDA particles loaded with ciprofloxacin (Figure 17 – A). Temperature induced drug release was evaluated from both loose drug loaded particles and those encased in alginate around a heating thread. The final vision is for the temperature induced drug release to be controlled by a microcontroller, however for this study water baths were utilized. Release was performed in pre-heated PBS solution and the results analyzed with the help of a pre-prepared calibration curve for ciprofloxacin and an Infinite M Nano, Tecan plate reader, using an excitation wavelength of 278nm and an emission wavelength of 450nm.

PNIPAM-PEGDA thermo-responsive micro particles were made with microfluidics. A microfluidic droplet generator was produced using photo lithography, during which molds

made of Su-8 were via photolithography were used to cast PDMS. The PDMS chips were subsequently treated with a plasma machine and attached to glass microscope slides.

An inner aqueous phase was made up of 1% w/v 2-hydroxy-4'-(2-hydroxyethoxy)-2-methylpropiophenone photo initiator, 10% w/v poly(n-isopropylacrylamide) (PNIPAM), distilled water, 10% w/v poly(ethylene glycol) diacrylate (PEGDA), 0.4%w/v BIS and 0.6%w/v APS (which was added last). The outer aqueous phase was made up of heavy mineral oil and 10%v/v Span 80. Each solution was stored in a syringe (with the aqueous phase covered by aluminium foil to protect from pre-mature UV exposure. A syringe pump (Harvard Apparatus PHD 2000) was used to control the flow of each solution, with the rate for the outer oil phase set to 25µL/min and the inner aqueous phase set to 2.5µL/min. After particle formation and upon leaving the microfluidic chip, the particles were exposed to intense UV of 20mW/cm^2 in a spiraling tube for cross-linking. The cross-linking coil was mounted directly on top of ice in order to avoid premature heating. Particles were then washed via centrifugation with a dish soap - distilled water mix once and then distilled water only, a further three times. To the wash the particles, 1mL of distilled water or the dish soap distilled water solution would be pipetted into the Eppendorf containing the newly formed particles and vortexed briefly before centrifugation to once again separate out the particles. The supernatant was then pipetted out and the cycle repeated. The particles were then lyophilized for 24 hours. Microscope images of the particles during formation and after UV curing can be seen in Figure 17 – A and B. Analyses of the particle image using ImageJ showed a normal distribution in particle size based on the diameter, as can be seen in Figure 17 – C.

The polydispersity index (PDI) was calculated according to equation 4 [68] and resulted in a PDI of 0.11. A PDI of less than 0.2 is commonly found to represent an acceptably homogenous distribution of particle size [69].

$$PDI = \frac{\sigma}{\bar{x}} \tag{4}$$

In equation 4, σ represents the standard deviation while x-bar denotes the mean.

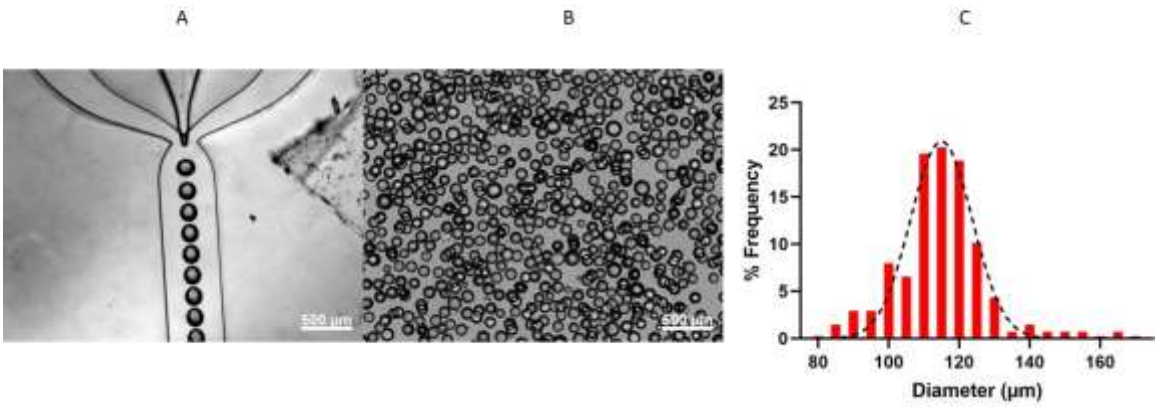

Figure 17: A) Microscope image of unloaded thermos-responsive PNIPAM-PEGDA micro particles. B) Histogram of particle size, demonstrating a gaussian distribution around a diameter of 114um.

In order to load the micro particles with drugs, a 1mg/mL solution of ciprofloxacin in distilled water was made. 15mg and 25mg of particles for the particle and alginate coating release studies respectively were placed Eppendorf tubes, before 1mL of the 1mg/mL ciprofloxacin solution was added. The particle – ciprofloxacin solutions were allowed to sit in the fridge at 8˚C for 24 hours. Due to the inverse thermo-responsive nature of PNIPAM-PEGDA particles they switch from hydrophilic to hydrophobic after crossing a temperature threshold of 32˚C. Due to this change in hydrophilicity the particles are able to either take up drug laced solution or expel the solution depending on the surrounding temperature. When cooled, the particles are in a hydrophilic state and fill with water infused

with ciprofloxacin, subsequently once heat is applied the particles change to hydrophobic, forcing any solution contained within out and in the process shrinking. After loading for 48 hours the particle containing solution was centrifuged and the supernatant extracted. The drug loaded particles were then washed 4 times in distilled water in order to remove any excess ciprofloxacin on the exterior of the particles.

In order to heat the drug loaded particles, they had to be suspended in an encasing material around the silver heating elements. Alginate was chosen as the encasing material because it is already approved by the Food and Drug Administration (FDA) for wound treatments and allows for the diffusion of drugs. In the final product, once drug delivery has been initiated the silver thread will be responsible for heating the drug delivery array with the help of an applied voltage by a microcontroller; however for the purposes of this project water baths were used to implement the correct temperatures with microcontroller controlled heating something that remains to be developed. The heat generated by the silver coated cotton thread will induce the change in hydrophilicity of the PNIPAM-PEGDA particles and force the loaded ciprofloxacin out into the alginate, from which it will diffuse into the adjacent wound bed.

In order to confirm the systems delivery of the drug in accordance with temperature both just the particles and particles coated in alginate around a silver coated thread were tested. The alginate coated drug release was also tested in a pulse release that will be discussed shortly. The release tests were performed at 3 different temperatures, namely 25 ˚C in a water bath, 37˚C carried out in a vacuum oven and 42˚C carried out in a water bath. Particles and particle – alginate mixtures cross-linked around silver coated threads were submerged in pre-heated PBS buffer, before having their temperature maintained via either

oven or water bath. Figure 18 – A shows the release profiles of PNIPAM-PEGDA particles on their own in 25˚C, 37˚C and 42˚C. At 25˚C a slow release of up to 25% of the maximum amount of drug is released, before a plateau is achieved. 37˚C follows a similar trend but with a higher peak of release at roughly 50% of the maximum release. Finally at 42˚C, the triggering temperature, a quick burst release is observed before a plateau whose difference from that of 25˚C and 37˚C is statistically significant. This study of the drug release profile of PNIPAM-PEGDA particles on their own demonstrates controlled release on demand, with higher levels of drug release with higher temperatures. As seen in Figure 18– B similar trends were observed when drug release with the alginate encasing around a heating thread was tested. Lower amounts of overall relative drug release were achieved, likely due to some of the ciprofloxacin remaining in the outer alginate coating. The alginate coating was both a hindrance and a help, in that it reduced the passive release (something to be avoided due to the rise in antibiotic resistant microorganisms) but it also reduced the peak amount of drug released when drug release was intended. The leakage of antibiotic represents an area in which significant improvement is needed, as premature release of antibiotics can lead to the development of antibiotic resistance.

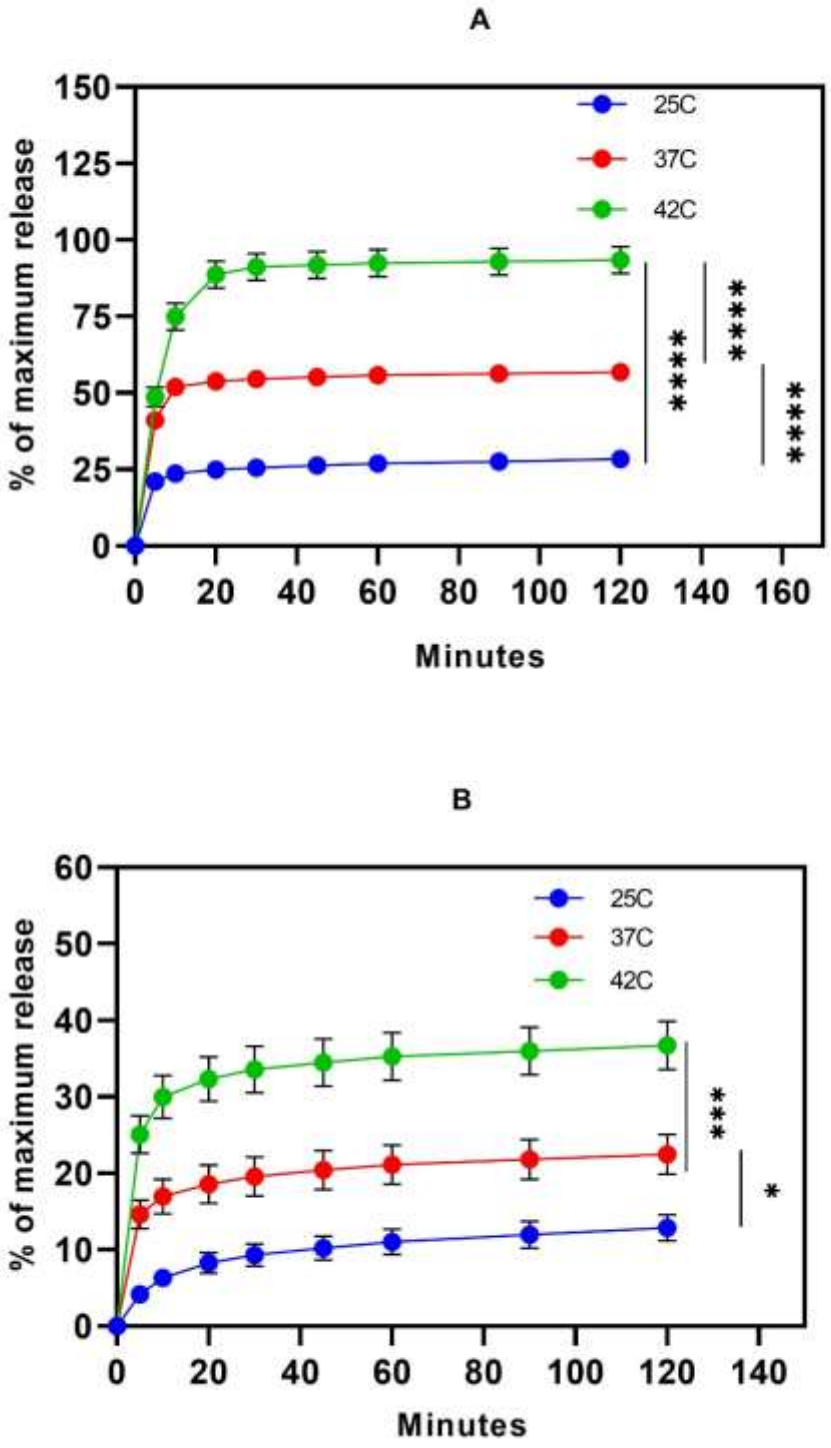

Figure 18: A) Ciprofloxacin release from loose PNIPAM-PEGDA particles. B) Ciprofloxacin release from alginate encased heating threads. Measurements were taken with an Infinite M Nano, Tecan plate reader, using an excitation wavelength of 278nm and an emission wavelength of 450nm. Error bars denote standard error with n = 3. *P-values: *<0.05, **<0.01, ***<0.001, ****<0.0001).*

To further demonstrate the on demand release of ciprofloxacin with the use of the PNIPAM-PEGDA micro particles a pulsatile release profile was made. Threads were encased in alginate containing drug loaded PNIPAM-PEGDA particles as before. The threads were immersed in PBS kept at 42˚C in a water bath for 5 minutes before cooling in room temperature in PBS for 25 minutes, the cycle was repeated 4 times, with the PBS collected after each change for analysis. Spikes in released ciprofloxacin are shown to correspond with spikes in temperature, as seen below in Figure 19. There was less overall release when compared to the continually heated samples discussed above. The reduction in drug release is expected as the particles spend much less time in their hydrophobic state. The big take away from Figure 19 is that drug release is triggered when heating is triggered but that the drug release plateaus when the system is cooled at room temperature for extended periods of time.

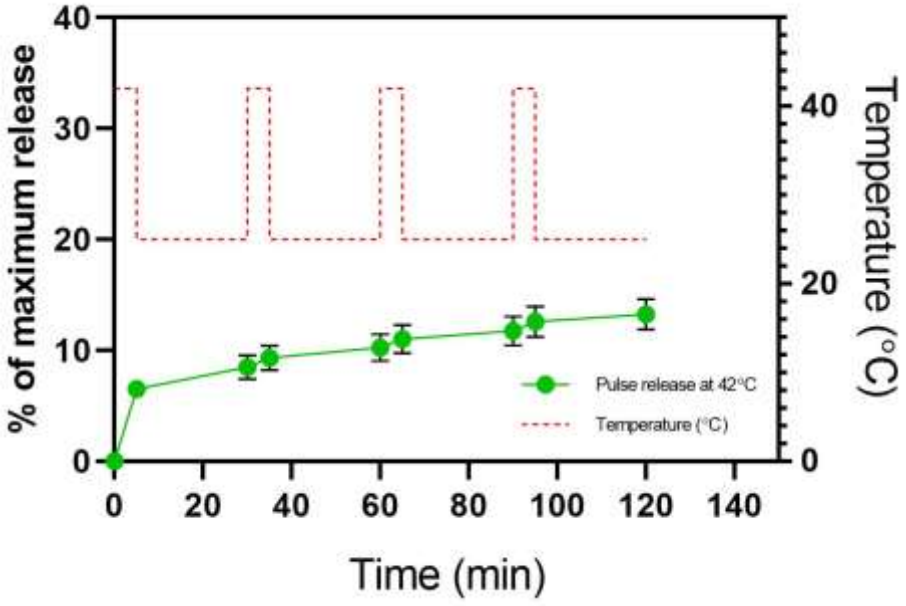

Figure 19: Pulse release of ciprofloxacin using 42˚C and room temperature. Error bars denote standard error with n = 3. P-values: *<0.05, **<0.01, ***<0.001, ****<0.0001).

Chapter 5: Biocompatibility

Biocompatibility of the system is crucial given its intended purpose for the treatment of burns. Depending on the degree of the burn some or all of the layers of the skin and underlying tissue can be damaged and exposed. In order to test the biocompatibility of our smart bandage components, in vitro cellular tests were conducted.

5.1 In Vitro Cell Studies

An in vitro biocompatibility test was performed according to ISO 10993-5, for the biological evaluation of medical devices [70]. Extracts of the materials in cell media were prepared according to ISO10993-12, whereby 0.1g of each type of thread were soaked in 1mL of cell media for 24, 72 and 168 hours long. Prior to soaking the thread samples in cell media they were extensively cleaned and sterilized in order to reduce the chance of contamination. Briefly the thread samples were washed three times in distilled water, followed by three washings in 70% ethanol and finally washed once again in water. The samples were then immersed in dulbecco's phosphate buffered saline (DPBS) overnight before UV sterilization for one hour on each side. HaCat cells were seeded into a 96 well plate with a cell density of 5000 cells per well and subsequently allowed to incubate for 24 hours. The cell media was then passaged with the contaminated media and incubated for a further 24 hours. After the final incubation and removal of the extract contaminated cell media, 110μL of cell media with 12μL of prestoBlue (Invitrogen by Thermofisher Scientific, Waltham, MA, USA) was allowed to incubate with the cells for a half hour. After the half hour incubation 100μL of the used cell media - prestoBlue solution was used to take a fluorescence intensity reading with excitation and emission wavelengths of 560nm and 590nm respectively using an Infinite M Nano, Tecan plate reader. ISO 10933-5 [70]

defines material to have a cytotoxic effect if they induce a drop of 30% in cell viability, which is observed in all of the samples after one week as shown in Figure 20-A. The carbon with silver base layer of carbon exhibited strong viability of 83% and 89% for one and three days, with no statistically significant difference between its viability and that of the control (as determined by a two way ANOVA conducted in Graph pad Prism software); However like both the silver and silver/silver chloride threads the cellular viability for silver coated in carbon dropped to roughly 17% cell viability after one week. Silver and silver/silver chloride demonstrated significant cytotoxic effects after one day, dropping immediately to around 17%. These results show that the silver compounds are the ones causing the cytotoxic effects and that the carbon acts as a shield for the silver in the base layer of the working and counter electrodes, at least for the first few days of use. The breakdown of the carbon and subsequent release of silver into the media, as shown by the drop in cell viability for cell media extract made over the course of a week, also potentially shows some insight into the gradual drop in signal in the midterm stability study, as a decomposition of the carbon material could reduce the signal.

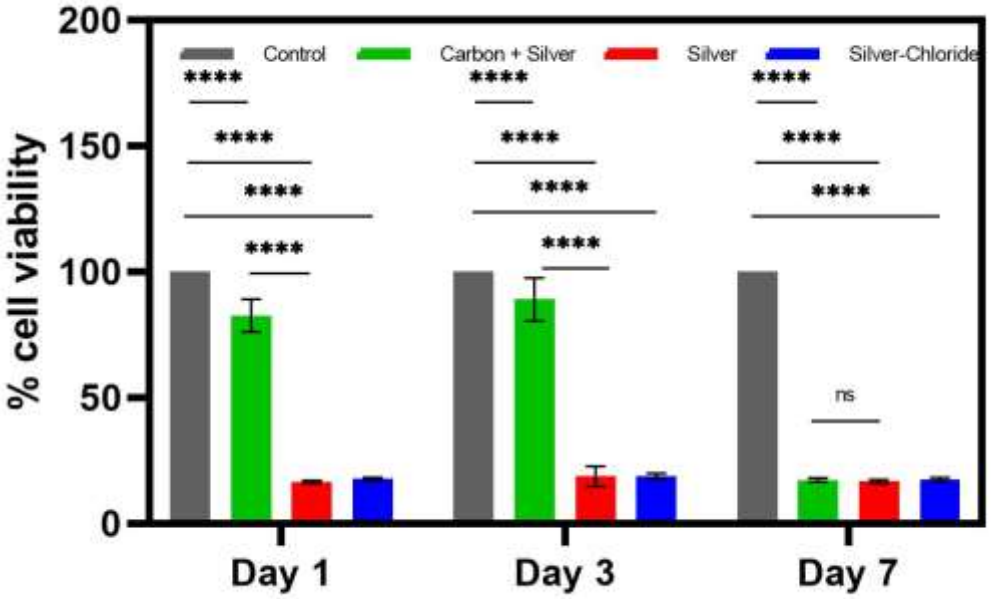

Figure 20: In vitro biocompatibility study for which HaCat cells were incubated in cell media used to soak cotton thread layered in the named material(s). Error bars denote standard deviation. P-values: *<0.05, **<0.01, ***<0.001, ****<0.0001).

5.2 Second in Vitro Cell Study

Another in vitro cell study using the same methodology as before was conducted but with smaller amounts of electrode material. 1cm lengths were chosen due to their future use in animal studies (due to size constraints), while 3cm lengths were chosen as that is the length at which the sensors have been characterized thus far.

As seen in Figure 21-A for the 1cm lengths there is no statistically significant difference between any of the materials and the control for up to three days. On day 7 there is a statistically significant difference between the control samples and the silver/silver chloride samples with a significant decrease in cell viability, but not enough for it to be called cytotoxic. In Figure 21-B showing the results for the 3cm long samples, the silver/silver chloride samples show significant cytotoxic effects by day 3, showing an ongoing issue

with biocompatibility. Before use in patients this issue needs to be improved so as not to cause more harm than good in patients.

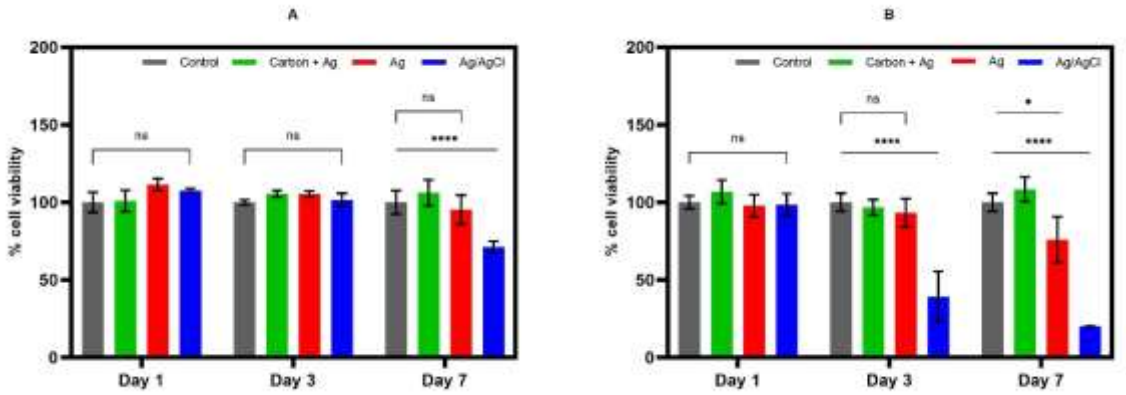

Figure 21: A) In vitro biocompatibility results for 1cm long samples, over 7 days. B) In vitro biocompatibility results for 3cm long samples, over 7 days.). Error bars denote standard deviation. P-values: *<0.05, **<0.01, ***<0.001, ****<0.0001).

5.3 Possible Solution to the Cytotoxic Nature of the Conductive Materials

In order to rectify the cytotoxic nature of the Silver Chloride material, as that is the Silver based compound exposed directly to the wound, a solution of polycaprolactone (PCL) was electro spun onto the reference electrodes. In brief 15 w/w% PCL (MW 45,000, Sigma Aldrich, USA) was dissolved in an 80:20 ratio of Dichloromethane (CH2Cl2, Sigma Aldrich, USA) and methanol (Fisher Chemical, USA). The solution was kept at constant agitation at room temperature for 2 hours, until the solution became homogeneous. The solution was loaded into a 10mL syringe, and an 18-gauge blunted needle was attached. The loaded syringes were then loaded into a programmable syringe pump (New Era Pump Systems, USA). The PCL coated threads were prepared using a customized electrospinning system where the syringe pump is elevated above a conductive base collector and the needle and base collector are attached to positive and negative terminals of a high voltage power supply (Gamma High Voltage Research, USA), respectively. Typically the thread

or material to be coated is moved and spooled while the dispensing needle is kept stationary. In this situation however the dupont pins had to already be attached to the relatively short reference electrodes (3cm), so the needle and syringe pump were moved during dispensing instead. The idea behind this porous biocompatible coating was to create separation between the Silver Chloride reference electrodes while still permitting wound exudate to come in contact with the electrode. Two aspects of these electro spun electrodes had to be tested, namely that the extra coating did not affect the signal and secondly that the coating did in fact improve biocompatibility. Shown below in Figure 22-A are the readings for 100µM with and without reference electrodes coated in PCL. The peaks reach roughly the same value and as can be seen in Figure 22-B no statistically significant difference as determined by Welch's T-test were found; however the standard deviation for the electrode sets using reference electrodes coated in PCL is noticeably increased.

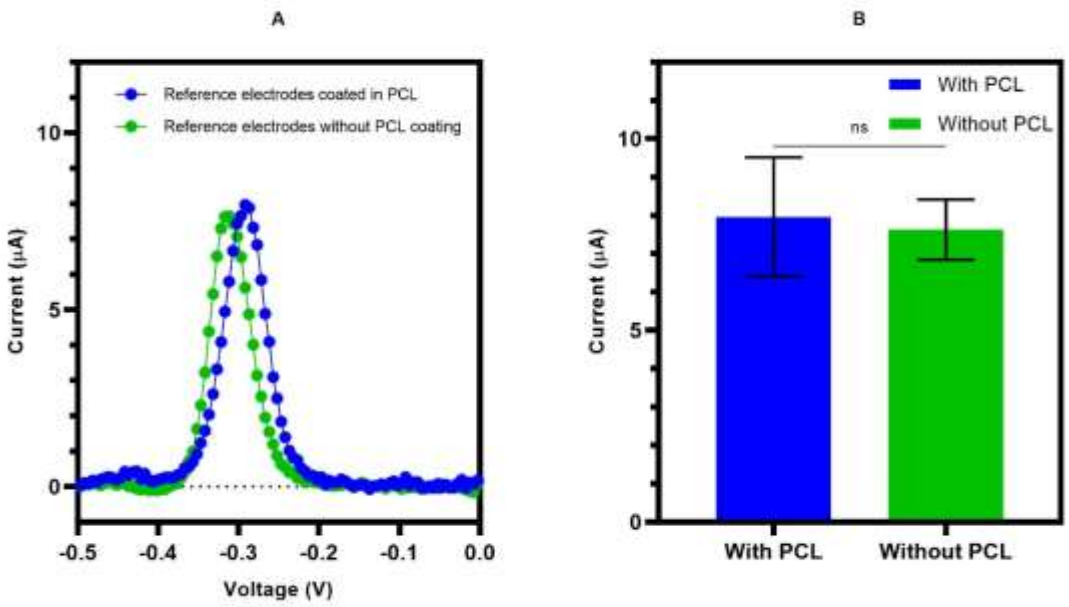

Figure 22: A) Comparing signal acquisition between sets of electrodes with and without reference electrodes coated in PCL. B) Comparing peak current values at -0.31V and -0.29V (Vs Ag/AgCl).

5.4 Further in Vitro Biocompatibility Studies

Now that it had been established that the PCL coating did not negatively affect the measurement of pyocyanin concentration in solution, further in vitro biocompatibility studies were undertaken to determine the effectiveness of the PCL coating in mitigating the cytotoxic effects of the silver-chloride. This study was carried out the same as for the previous in vitro biocompatibility study but of course with new materials. As seen below in Figure 23 the result for the PCL coated silver/silver chloride thread was much improved with significant increases in biocompatibility. Both 1 and 3cm long samples showed increased cell biocompatibility, with the 1cm long samples displaying no cytotoxic results over the course of the week; the 3cm long samples displayed positive results for the first 3 days and mixed results on day 7. Due to the nature of the tests performed the thread was fully immersed for 24 hours and the cells directly exposed to the extract obtained through this method. In clinical use the thread could be in contact with the wound bed but the PCL would in theory keep the silver chloride from direct contact with the patient's tissue while still allowing wound exudate to come in contact with the electrode, creating somewhat of a buffer between the silver/silver chloride and underlying tissue. The results show significant improvement, in terms of biocompatibility, with the additional layering of PCL, however further investigation of the 3cm long day 7 sample is required as well as further validation in in vivo wound models.

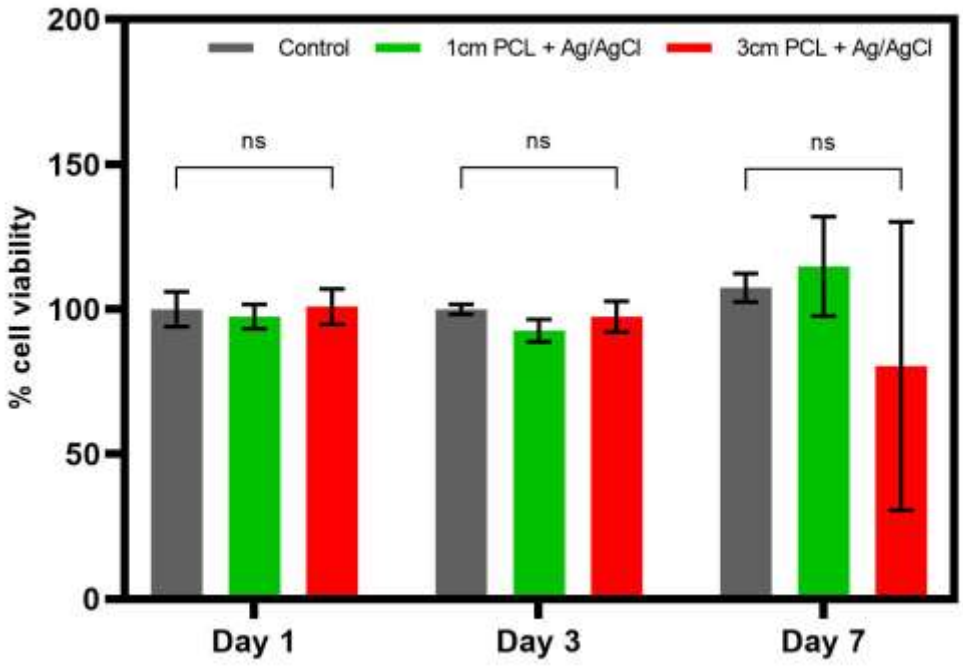

Figure 23: Carbon and PCL coated silver/silver chloride biocompatibility studies. Error bars denote standard deviation with n = 3. P-values: *<0.05, **<0.01, ***<0.001, ****<0.0001).

6.0 Conclusion and Future Work

The potential for a smart, bacteria specific, wound dressing system that can be integrated with existing treatment options for burn patients has been developed and shown. Affordable cotton thread based electrochemical sensors were developed and extensively tested in conjunction with an open-source potentiostat. The sensors demonstrated a linear response with an r-squared value of 0.9825 under ideal conditions. Under non-ideal conditions the sensors were shown to be able to detect pyocyanin in a variety of solutions and circumstances, including while the electrodes were woven into medical gauze and detecting pyocyanin in a bacterial culture. Sensor signal stability, an important concern was also demonstrated with only small, statistically insignificant, deviations in signal strength over 24 hours of immersion. Over the course of a week of continual use the signal strength demonstrated a gradual decline, with a statistically significant difference between day 1 and day 7. The degradation is likely do to decomposition of the electrode material but warrants further investigation. While the signal does degrade, it is still possible to get a positive identification of pyocyanin even after 7 days of use. The final portion of the stability study, the long term stability of the sensors, their shelf-life for lack of a better word, is part of the future work and is currently underway. Another possible test to carry out is simply immersing some sets of sensors in a pyocyanin solution for one, three and seven days before taking readings.

The sensors ability to detect pyocyanin in adverse conditions was evaluated and found to function well. A signal for pyocyanin could easily be distinguished while in solution with both used and unused cell media, ciprofloxacin and silver sulfadiazine.

Real time, effective control of drug storage and release was demonstrated through the use of PNIPAM-PEGDA micro particles, enmeshed in crosslinked alginate and coated on Silver coated cotton threads. Controlled release of ciprofloxacin based on temperature for loose PNIPAM-PEDGA particles was demonstrated with significant statistical differences noted between room temperature, body temperature and 42˚C. A similar trend was observed for the drug release profile of particles encased with alginate around a heating element thread. For this study the heating elements were tested with the use of ovens and water baths, mostly looking at the drug release of the particles through the alginate, significant characterization of the heating threads themselves and the microcontroller utilized to heat them is still required. The amount of voltage and the duty cycle used to heat the heating threads will need to be explored in depth for accurate, precise control over the temperature.

The thread based technologies effectiveness and ability to be integrated with current medical dressings was proven with in-vitro bacterial cultures and the detection of pyocyanin while thread based electrodes were woven into standard medical gauze.

Perhaps the biggest challenge facing this work is the biocompatibility. The initial cell viability study revealed that the silver compounds involved in this work carried a large cytotoxic effect, however 13 times more material was used in those tests than is supposed to go on an actual wound. A secondary in vitro study was carried out using the same protocol but with significantly less sample material, more in line with what is intended for use in the field (1 and 3cm long samples). The secondary study showed much less cytotoxic behaviour with only the 3cm long silver/silver chloride and to a lesser degree the 3cm silver samples displaying this property. The Silver heating elements encased in alginate have

already appeared in an animal study carried out by Lucas et al. [61] in which tissue staining revealed no inflammatory response and re-epithelization; however no in-vitro cytotoxicity/cell viability study was conducted for silver encased in alginate and containing ciprofloxacin loaded PNIPAM-PEGDA micro particles, something that will need to be evaluated in the future. Since the alginate coating seems to not produce significant biocompatibility issues, at least in the animal model, a possible solution for the carbon and silver electrodes as well as the silver/silver chloride reference electrodes could be an extra coating with a biologically inert and porous material such as PCL. This theory was tested with several silver/silver chloride reference electrodes being coated in PCL using an electro spinner. The measurements taken with the PCL coated reference electrodes were in accordance with readings taken previously and didn't impact the peak current level in any significant way. The reference electrodes coated in PCL had their cytotoxicity re-evaluated in vitro with smaller amounts of material (1 and 3cm long). The results showed much improved biocompatibility with the only negative effects being observed for the 3cm long samples after 7 days. Another possible coating that could improve the biocompatibility is one of polyethylene glycol diacrylate (PEDGA). The Silver heating elements are unlikely to cause significant issue in the long run as they will ultimately be encased in alginate.

Lastly the development and integration of more thread sensors and drug delivery systems into a compact, inexpensive package will be undertaken. This work has demonstrated the ability to produce bacteria specific sensing systems cheaply; combining the electrical systems involved in this project with those needed for other forms of measurement, such as temperature and pH to name but a few, into one small low cost package with a multitude of sensing and treatment options available would represent a major step forward in caring

for burn victims. In terms of specifically targeting *P. aeruginosa* the analysis of pyoverdine using the same setup as described in this thesis should be undertaken. Pyoverdine is another redox active virulence factor unique to *P. aeruginosa* that can be detected using the same technique of SWV, but it has a peak in the positive voltage range at 0.4V. Pyoverdine can be used for additional confirmation as to the presence of *P. aeruginosa* in a burn wound using the same sensors developed in this study. Redox active compounds unique to other bacteria could potentially also serve as rapidly detectable biomarkers and warrant further investigation.

Bibliography

[1] "Burns." http://www.who.int/news-room/fact-sheets/detail/burns (accessed Jul. 05, 2020).

[2] "Appendix 3 Type of most serious injury among people who sustained at least one activity-limiting injury during the past 12 months, population aged 12 and over, Canada, 2009–2010." https://www150.statcan.gc.ca/n1/pub/82-624-x/2011001/article/app/11506-03-app3-eng.htm (accessed Feb. 25, 2020).

[3] "Classification of Burns - Health Encyclopedia - University of Rochester Medical Center." https://www.urmc.rochester.edu/encyclopedia/content.aspx?ContentTypeID=90&ContentID=P09575 (accessed Jul. 05, 2020).

[4] S. Hettiaratchy and P. Dziewulski, "Pathophysiology and types of burns," *BMJ*, vol. 328, no. 7453, pp. 1427–1429, Jun. 2004.

[5] P. H. A. of Canada, "Emergency department surveillance of burns and scalds, electronic Canadian Hospitals Injury Reporting and Prevention Program, 2013 - HPCDP: Volume 37-1, January 2017," *aem*, Jan. 01, 2017. https://www.canada.ca/en/public-health/services/reports-publications/health-promotion-chronic-disease-prevention-canada-research-policy-practice/vol-37-no-1-2017/glance-emergency-department-surveillance-thermal-burns-scalds-electronic-canadian-hospitals-injury-reporting-prevention-program-2013.html (accessed Jul. 05, 2020).

[6] P. H. A. of Canada, “The Cost of Injury in Canada,” *gcnws*, Nov. 24, 1998. https://www.canada.ca/en/public-health/services/injury-prevention/cost-injury-canada.html (accessed Jul. 05, 2020).

[7] D. Church, S. Elsayed, O. Reid, B. Winston, and R. Lindsay, “Burn Wound Infections,” *Clin. Microbiol. Rev.*, vol. 19, no. 2, pp. 403–434, Apr. 2006, doi: 10.1128/CMR.19.2.403-434.2006.

[8] P. Shakespeare, “Burn wound healing and skin substitutes,” *Burns*, vol. 27, no. 5, pp. 517–522, Aug. 2001, doi: 10.1016/S0305-4179(01)00017-1.

[9] M. G. Jeschke, M. E. van Baar, M. A. Choudhry, K. K. Chung, N. S. Gibran, and S. Logsetty, “Burn injury,” *Nat. Rev. Dis. Primer*, vol. 6, no. 1, 2020, doi: 10.1038/s41572-020-0145-5.

[10] M. P. Rowan *et al.*, “Burn wound healing and treatment: review and advancements,” *Crit. Care*, vol. 19, 2015, doi: 10.1186/s13054-015-0961-2.

[11] S. Werner, T. Krieg, and H. Smola, “Keratinocyte–Fibroblast Interactions in Wound Healing,” *J. Invest. Dermatol.*, vol. 127, no. 5, pp. 998–1008, May 2007, doi: 10.1038/sj.jid.5700786.

[12] W. Wu, Y. Jin, F. Bai, and S. Jin, “Chapter 41 - Pseudomonas aeruginosa,” in *Molecular Medical Microbiology (Second Edition)*, Y.-W. Tang, M. Sussman, D. Liu, I. Poxton, and J. Schwartzman, Eds. Boston: Academic Press, 2015, pp. 753–767.

[13] E. E. Tredget, H. A. Shankowsky, R. Rennie, R. E. Burrell, and S. Logsetty, “Pseudomonas infections in the thermally injured patient,” *Burns*, vol. 30, no. 1, pp. 3–26, Feb. 2004, doi: 10.1016/j.burns.2003.08.007.

[14] A. T. McManus, A. D. Mason, W. F. McManus, and B. A. Pruitt, “Twenty-five year review ofPseudomonas aeruginosa bacteremia in a burn center,” *Eur. J. Clin. Microbiol.*, vol. 4, no. 2, pp. 219–223, Apr. 1985, doi: 10.1007/BF02013601.

[15] M. R. Gonzalez *et al.*, “Effect of Human Burn Wound Exudate on Pseudomonas aeruginosa Virulence,” *mSphere*, vol. 1, no. 2, Apr. 2016, doi: 10.1128/mSphere.00111-15.

[16] “WHO | Publications,” *WHO*. http://www.who.int/surgery/publications/en/ (accessed Feb. 28, 2020).

[17] M. Z. El-Fouly, A. M. Sharaf, A. A. M. Shahin, H. A. El-Bialy, and A. M. A. Omara, “Biosynthesis of pyocyanin pigment by Pseudomonas aeruginosa,” *J. Radiat. Res. Appl. Sci.*, vol. 8, no. 1, pp. 36–48, Jan. 2015, doi: 10.1016/j.jrras.2014.10.007.

[18] G. W. Lau, D. J. Hassett, H. Ran, and F. Kong, “The role of pyocyanin in Pseudomonas aeruginosa infection,” *Trends Mol. Med.*, vol. 10, no. 12, pp. 599–606, Dec. 2004, doi: 10.1016/j.molmed.2004.10.002.

[19] L. R. Usher *et al.*, “Induction of neutrophil apoptosis by the Pseudomonas aeruginosa exotoxin pyocyanin: a potential mechanism of persistent infection,” *J. Immunol. Baltim. Md 1950*, vol. 168, no. 4, pp. 1861–1868, Feb. 2002, doi: 10.4049/jimmunol.168.4.1861.

[20] L. Allen *et al.*, “Pyocyanin production by Pseudomonas aeruginosa induces neutrophil apoptosis and impairs neutrophil-mediated host defenses in vivo,” *J. Immunol. Baltim. Md 1950*, vol. 174, no. 6, pp. 3643–3649, Mar. 2005, doi: 10.4049/jimmunol.174.6.3643.

[21] T. A. Webster, H. J. Sismaet, J. L. Conte, I. J. Chan, and E. D. Goluch, "Electrochemical detection of Pseudomonas aeruginosa in human fluid samples via pyocyanin," *Biosens. Bioelectron.*, vol. 60, pp. 265–270, Oct. 2014, doi: 10.1016/j.bios.2014.04.028.

[22] H. Ran, D. J. Hassett, and G. W. Lau, "Human targets of Pseudomonas aeruginosa pyocyanin," *Proc. Natl. Acad. Sci.*, vol. 100, no. 24, pp. 14315–14320, Nov. 2003, doi: 10.1073/pnas.2332354100.

[23] Y. Q. O'Malley, M. Y. Abdalla, M. L. McCormick, K. J. Reszka, G. M. Denning, and B. E. Britigan, "Subcellular localization of Pseudomonas pyocyanin cytotoxicity in human lung epithelial cells," *Am. J. Physiol.-Lung Cell. Mol. Physiol.*, vol. 284, no. 2, pp. L420–L430, Feb. 2003, doi: 10.1152/ajplung.00316.2002.

[24] L. R. Usher *et al.*, "Induction of Neutrophil Apoptosis by the Pseudomonas aeruginosa Exotoxin Pyocyanin: A Potential Mechanism of Persistent Infection," *J. Immunol.*, vol. 168, no. 4, pp. 1861–1868, Feb. 2002, doi: 10.4049/jimmunol.168.4.1861.

[25] S. Hall *et al.*, "Cellular Effects of Pyocyanin, a Secreted Virulence Factor of Pseudomonas aeruginosa," *Toxins*, vol. 8, no. 8, Aug. 2016, doi: 10.3390/toxins8080236.

[26] H. J. Sismaet, A. J. Pinto, and E. D. Goluch, "Electrochemical sensors for identifying pyocyanin production in clinical Pseudomonas aeruginosa isolates," *Biosens. Bioelectron.*, vol. 97, pp. 65–69, Nov. 2017, doi: 10.1016/j.bios.2017.05.042.

[27] J. F. Parsons, B. T. Greenhagen, K. Shi, K. Calabrese, H. Robinson, and J. E. Ladner, "Structural and Functional Analysis of the Pyocyanin Biosynthetic Protein PhzM from Pseudomonas aeruginosa," *Biochemistry*, vol. 46, no. 7, pp. 1821–1828, Feb. 2007, doi: 10.1021/bi6024403.

[28] O. Simoska *et al.*, "Real-Time Electrochemical Detection of Pseudomonas aeruginosa Phenazine Metabolites Using Transparent Carbon Ultramicroelectrode Arrays," *ACS Sens.*, vol. 4, no. 1, pp. 170–179, Jan. 2019, doi: 10.1021/acssensors.8b01152.

[29] D. V. Mavrodi, R. F. Bonsall, S. M. Delaney, M. J. Soule, G. Phillips, and L. S. Thomashow, "Functional Analysis of Genes for Biosynthesis of Pyocyanin and Phenazine-1-Carboxamide from Pseudomonas aeruginosa PAO1," *J. Bacteriol.*, vol. 183, no. 21, pp. 6454–6465, Nov. 2001, doi: 10.1128/JB.183.21.6454-6465.2001.

[30] R. M. Donlan, "Biofilms: Microbial Life on Surfaces," *Emerg. Infect. Dis.*, vol. 8, no. 9, pp. 881–890, Sep. 2002, doi: 10.3201/eid0809.020063.

[31] H.-C. Flemming and J. Wingender, "The biofilm matrix," *Nat. Rev. Microbiol.*, vol. 8, no. 9, pp. 623–633, Sep. 2010, doi: 10.1038/nrmicro2415.

[32] I. W. Sutherland, "The biofilm matrix – an immobilized but dynamic microbial environment," *Trends Microbiol.*, vol. 9, no. 5, pp. 222–227, May 2001, doi: 10.1016/S0966-842X(01)02012-1.

[33] T. Rasamiravaka, Q. Labtani, P. Duez, and M. El Jaziri, "The Formation of Biofilms by Pseudomonas aeruginosa: A Review of the Natural and Synthetic Compounds Interfering with Control Mechanisms," *BioMed Research International*,

2015. https://www.hindawi.com/journals/bmri/2015/759348/ (accessed Mar. 27, 2020).

[34] L. Ma, M. Conover, H. Lu, M. R. Parsek, K. Bayles, and D. J. Wozniak, "Assembly and Development of the Pseudomonas aeruginosa Biofilm Matrix," *PLoS Pathog.*, vol. 5, no. 3, Mar. 2009, doi: 10.1371/journal.ppat.1000354.

[35] L. R. Mulcahy, V. M. Isabella, and K. Lewis, "Pseudomonas aeruginosa biofilms in disease," *Microb. Ecol.*, vol. 68, no. 1, pp. 1–12, Jul. 2014, doi: 10.1007/s00248-013-0297-x.

[36] M. F. Moradali, S. Ghods, and B. H. A. Rehm, "Pseudomonas aeruginosa Lifestyle: A Paradigm for Adaptation, Survival, and Persistence," *Front. Cell. Infect. Microbiol.*, vol. 7, 2017, doi: 10.3389/fcimb.2017.00039.

[37] E. Olivares, S. Badel-Berchoux, C. Provot, G. Prévost, T. Bernardi, and F. Jehl, "Clinical Impact of Antibiotics for the Treatment of Pseudomonas aeruginosa Biofilm Infections," *Front. Microbiol.*, vol. 10, 2020, doi: 10.3389/fmicb.2019.02894.

[38] C.-Y. Chang, "Surface Sensing for Biofilm Formation in Pseudomonas aeruginosa," *Front. Microbiol.*, vol. 8, Jan. 2018, doi: 10.3389/fmicb.2017.02671.

[39] P. A. Suci, M. W. Mittelman, F. P. Yu, and G. G. Geesey, "Investigation of ciprofloxacin penetration into Pseudomonas aeruginosa biofilms.," *Antimicrob. Agents Chemother.*, vol. 38, no. 9, pp. 2125–2133, Sep. 1994, doi: 10.1128/AAC.38.9.2125.

[40] R. Donlan, "Role of Biofilms in Antimicrobial Resistance," *Asaio J.*, vol. 46, no. 6, Dec. 2000, Accessed: Mar. 27, 2020. [Online]. Available: insights.ovid.com.

[41] D. M. Campoli-Richards, J. P. Monk, A. Price, P. Benfield, P. A. Todd, and A. Ward, “Ciprofloxacin,” *Drugs*, vol. 35, no. 4, pp. 373–447, Apr. 1988, doi: 10.2165/00003495-198835040-00003.

[42] T. D. M. Pham, Z. M. Ziora, and M. A. T. Blaskovich, “Quinolone antibiotics,” *MedChemComm*, vol. 10, no. 10, pp. 1719–1739, Jun. 2019, doi: 10.1039/c9md00120d.

[43] X. S. Pan, J. Ambler, S. Mehtar, and L. M. Fisher, “Involvement of topoisomerase IV and DNA gyrase as ciprofloxacin targets in Streptococcus pneumoniae.,” *Antimicrob. Agents Chemother.*, vol. 40, no. 10, pp. 2321–2326, Oct. 1996.

[44] N. R. Cozzarelli, “DNA gyrase and the supercoiling of DNA,” *Science*, vol. 207, no. 4434, pp. 953–960, Feb. 1980, doi: 10.1126/science.6243420.

[45] L. S. Redgrave, S. B. Sutton, M. A. Webber, and L. J. V. Piddock, “Fluoroquinolone resistance: mechanisms, impact on bacteria, and role in evolutionary success,” *Trends Microbiol.*, vol. 22, no. 8, pp. 438–445, Aug. 2014, doi: 10.1016/j.tim.2014.04.007.

[46] D. Sharp, P. Gladstone, R. B. Smith, S. Forsythe, and J. Davis, “Approaching intelligent infection diagnostics: Carbon fibre sensor for electrochemical pyocyanin detection,” *Bioelectrochemistry*, vol. 77, no. 2, pp. 114–119, Feb. 2010, doi: 10.1016/j.bioelechem.2009.07.008.

[47] “CH Instruments Potentiostats.” http://www.ijcambria-webshop.com/images/mall/ppage6.aspx (accessed Jul. 17, 2020).

[48] B. Ciui, M. Tertiş, A. Cernat, R. Săndulescu, J. Wang, and C. Cristea, “Finger-Based Printed Sensors Integrated on a Glove for On-Site Screening Of Pseudomonas

aeruginosa Virulence Factors," *Anal. Chem.*, vol. 90, no. 12, pp. 7761–7768, Jun. 2018, doi: 10.1021/acs.analchem.8b01915.

[49] J. Kim, A. S. Campbell, B. E.-F. de Ávila, and J. Wang, "Wearable biosensors for healthcare monitoring," *Nat. Biotechnol.*, vol. 37, no. 4, Art. no. 4, Apr. 2019, doi: 10.1038/s41587-019-0045-y.

[50] A. J. Bandodkar, I. Jeerapan, and J. Wang, "Wearable Chemical Sensors: Present Challenges and Future Prospects," *ACS Sens.*, vol. 1, no. 5, pp. 464–482, May 2016, doi: 10.1021/acssensors.6b00250.

[51] R. K. Mishra *et al.*, "Wearable Flexible and Stretchable Glove Biosensor for On-Site Detection of Organophosphorus Chemical Threats," *ACS Sens.*, vol. 2, no. 4, pp. 553–561, Apr. 2017, doi: 10.1021/acssensors.7b00051.

[52] P. Mostafalu *et al.*, "Smart Bandage for Monitoring and Treatment of Chronic Wounds," *Small*, vol. 14, no. 33, p. 1703509, 2018, doi: 10.1002/smll.201703509.

[53] B. Mirani *et al.*, "An Advanced Multifunctional Hydrogel-Based Dressing for Wound Monitoring and Drug Delivery," *Adv. Healthc. Mater.*, vol. 6, no. 19, p. 1700718, 2017, doi: 10.1002/adhm.201700718.

[54] W. Gao *et al.*, "Fully integrated wearable sensor arrays for multiplexed in situ perspiration analysis," *Nature*, vol. 529, no. 7587, Art. no. 7587, Jan. 2016, doi: 10.1038/nature16521.

[55] P. Mostafalu, M. Akbari, K. A. Alberti, Q. Xu, A. Khademhosseini, and S. R. Sonkusale, "A toolkit of thread-based microfluidics, sensors and electronics for 3D tissue embedding for medical diagnostics," *Microsyst. Nanoeng.*, vol. 2, no. 1, Dec. 2016, doi: 10.1038/micronano.2016.39.

[56] R. Rahimi *et al.*, "A low-cost flexible pH sensor array for wound assessment," *Sens. Actuators B Chem.*, vol. 229, pp. 609–617, Jun. 2016, doi: 10.1016/j.snb.2015.12.082.

[57] A. Ainla *et al.*, "Open-Source Potentiostat for Wireless Electrochemical Detection with Smartphones," *Anal. Chem.*, vol. 90, no. 10, pp. 6240–6246, May 2018, doi: 10.1021/acs.analchem.8b00850.

[58] M. Bassetti, A. Vena, A. Croxatto, E. Righi, and B. Guery, "How to manage Pseudomonas aeruginosa infections," *Drugs Context*, vol. 7, May 2018, doi: 10.7573/dic.212527.

[59] V. Gubala, L. F. Harris, A. J. Ricco, M. X. Tan, and D. E. Williams, "Point of Care Diagnostics: Status and Future," *Anal. Chem.*, vol. 84, no. 2, pp. 487–515, Jan. 2012, doi: 10.1021/ac2030199.

[60] T. R. Kozel and A. R. Burnham-Marusich, "Point-of-Care Testing for Infectious Diseases: Past, Present, and Future," *J. Clin. Microbiol.*, vol. 55, no. 8, pp. 2313–2320, Aug. 2017, doi: 10.1128/JCM.00476-17.

[61] L. Karperien, "pH sensitive thread-based wound dressing with integrated drug delivery and wireless bluetooth interface," Thesis, 2019.

[62] M. Muller, Z. Li, and P. K. M. Maitz, "Pseudomonas pyocyanin inhibits wound repair by inducing premature cellular senescence: Role for p38 mitogen-activated protein kinase," *Burns*, vol. 35, no. 4, pp. 500–508, Jun. 2009, doi: 10.1016/j.burns.2008.11.010.

[63] D. A. Armbruster and T. Pry, "Limit of Blank, Limit of Detection and Limit of Quantitation," *Clin. Biochem. Rev.*, vol. 29, no. Suppl 1, pp. S49–S52, Aug. 2008.

[64] P. Gayen and B. P. Chaplin, “Selective Electrochemical Detection of Ciprofloxacin with a Porous Nafion/Multiwalled Carbon Nanotube Composite Film Electrode,” *ACS Appl. Mater. Interfaces*, vol. 8, no. 3, pp. 1615–1626, Jan. 2016, doi: 10.1021/acsami.5b07337.

[65] L. Fotouhi and M. Alahyari, “Electrochemical behavior and analytical application of ciprofloxacin using a multi-walled nanotube composite film-glassy carbon electrode,” *Colloids Surf. B Biointerfaces*, vol. 81, no. 1, pp. 110–114, Nov. 2010, doi: 10.1016/j.colsurfb.2010.06.030.

[66] G. S. Garbellini, R. C. Rocha-Filho, and O. Fatibello-Filho, “Voltammetric determination of ciprofloxacin in urine samples and its interaction with dsDNA on a cathodically pretreated boron-doped diamond electrode,” *Anal. Methods*, vol. 7, no. 8, pp. 3411–3418, Apr. 2015, doi: 10.1039/C5AY00625B.

[67] G. Grant, T. Zhang, L. Gloyne, A. Perkins, M. Kiefel, and S. Anoopkumar-Dukie, “Exogenous Pyocyanin Alters Pseudomonas aeruginosa Susceptibility to Ciprofloxacin,” Jan. 2010.

[68] Q. Xu *et al.*, “Preparation of Monodisperse Biodegradable Polymer Microparticles Using a Microfluidic Flow-Focusing Device for Controlled Drug Delivery,” *Small*, vol. 5, no. 13, pp. 1575–1581, 2009, doi: 10.1002/smll.200801855.

[69] M. Danaei *et al.*, “Impact of Particle Size and Polydispersity Index on the Clinical Applications of Lipidic Nanocarrier Systems,” *Pharmaceutics*, vol. 10, no. 2, May 2018, doi: 10.3390/pharmaceutics10020057.

[70] 14:00-17:00, “ISO 10993-5:2009,” *ISO*. https://www.iso.org/cms/render/live/en/sites/isoorg/contents/data/standard/03/64/36406.html (accessed Apr. 12, 2020).